JBMR Plus, 2024, **8**, ziae051
https://doi.org/10.1093/jbmrpl/ziae051
Advance access publication: April 10, 2024
Research Article

Osteoporosis GWAS-implicated *DNM3* locus contextually regulates osteoblastic and chondrogenic fate of mesenchymal stem/progenitor cells through oscillating miR-199a-5p levels

Gurcharan Kaur[1], James A. Pippin[2], Solomon Chang[3], Justin Redmond[1,3], Alessandra Chesi[2,4,5], Andrew D. Wells[2,5], Tristan Maerz[3], Struan F.A. Grant[2,4,6,7,8,9], Rhima M. Coleman[1,3], Kurt D. Hankenson[1,3,*], Yadav Wagley[3,*]

[1]Department of Biomedical Engineering, University of Michigan Medical School, Ann Arbor, MI 48109, United States
[2]Center for Spatial and Functional Genomics, The Children's Hospital of Philadelphia, Philadelphia, PA 19104, United States
[3]Department of Orthopaedic Surgery, University of Michigan Medical School, Ann Arbor, MI 48109, United States
[4]Division of Human Genetics, The Children's Hospital of Philadelphia, Philadelphia, PA 19104, United States
[5]Department of Pathology and Laboratory Medicine, Perelman School of Medicine, University of Pennsylvania, Philadelphia, PA 19104, United States
[6]Division of Diabetes and Endocrinology, The Children's Hospital of Philadelphia, Philadelphia, PA 19104, United States
[7]Department of Pediatrics, Perelman School of Medicine, University of Pennsylvania, Philadelphia, PA 19104, United States
[8]Institute of Diabetes, Obesity and Metabolism, Perelman School of Medicine, University of Pennsylvania, Philadelphia, PA 19104, United States
[9]Department of Genetics, Perelman School of Medicine, University of Pennsylvania, Philadelphia, PA 19104, United States

*Corresponding authors: Yadav Wagley, Department of Orthopaedic Surgery, University of Michigan Medical School, 109 Zina Pitcher Pl, Rm 2019 Biomedical Sciences Research Building, University of Michigan Medical School, Ann Arbor, MI 48109, United States (ywagley@med.umich.edu); Kurt D. Hankenson, Department of Orthopaedic Surgery, University of Michigan Medical School, 109 Zina Pitcher Pl, Rm 2019 Biomedical Sciences Research Building, University of Michigan Medical School, Ann Arbor, MI 48109, United States (kdhank@umich.edu)

Abstract

Genome wide association study (GWAS)-implicated bone mineral density (BMD) signals have been shown to localize in cis-regulatory regions of distal effector genes using 3D genomic methods. Detailed characterization of such genes can reveal novel causal genes for BMD determination. Here, we elected to characterize the "*DNM3*" locus on chr1q24, where the long non-coding RNA *DNM3OS* and the embedded microRNA *MIR199A2* (miR-199a-5p) are implicated as effector genes contacted by the region harboring variation in linkage disequilibrium with BMD-associated sentinel single nucleotide polymorphism, rs12041600. During osteoblast differentiation of human mesenchymal stem/progenitor cells (hMSC), miR-199a-5p expression was temporally decreased and correlated with the induction of osteoblastic transcription factors RUNX2 and Osterix. Functional relevance of miR-199a-5p downregulation in osteoblastogenesis was investigated by introducing miR-199a-5p mimic into hMSC. Cells overexpressing miR-199a-5p depicted a cobblestone-like morphological change and failed to produce BMP2-dependent extracellular matrix mineralization. Mechanistically, a miR-199a-5p mimic modified hMSC propagated normal SMAD1/5/9 signaling and expressed osteoblastic transcription factors RUNX2 and Osterix but depicted pronounced upregulation of SOX9 and enhanced expression of essential chondrogenic genes *ACAN, COMP,* and *COL10A1*. Mineralization defects, morphological changes, and enhanced chondrogenic gene expression associated with miR-199a-5p mimic over-expression were restored with miR-199a-5p inhibitor suggesting specificity of miR-199a-5p in chondrogenic fate specification. The expression of both the *DNM3OS* and miR-199a-5p temporally increased and correlated with hMSC chondrogenic differentiation. Although miR-199a-5p overexpression failed to further enhance chondrogenesis, blocking miR-199a-5p activity significantly reduced chondrogenic pellet size, extracellular matrix deposition, and chondrogenic gene expression. Taken together, our results indicate that oscillating miR-199a-5p levels dictate hMSC osteoblast or chondrocyte terminal fate. Our study highlights a functional role of miR-199a-5p as a BMD effector gene at the *DNM3* BMD GWAS locus, where patients with cis-regulatory genetic variation which increases miR-199a-5p expression could lead to reduced osteoblast activity.

Keywords: DNM3OS, miR-199a-5p, bone morphogenetic protein, human mesenchymal stem cells, osteoblasts, chondrocytes

Lay Summary

Genome wide association study (GWAS) implicated candidate causal variants principally reside in non-coding regulatory regions of the genome and can influence the cis expression of effector genes from relatively large distances. Many of these phenomena are specific to cellular context and can be determined through 3-dimensional genomic approaches. Functional characterization to define the impact of putative candidate effector genes on bone cell differentiation is a necessary first step in functionalizing GWAS discoveries to understand phenotypic variation. We previously implicated miR-199a-5p embedded in the long non-coding RNA *DNM3OS* as bone mineral density (BMD) effector gene at the *DNM3*

Received: October 1, 2023. **Revised:** February 15, 2024. **Accepted:** April 11, 2024

GWAS locus. The osteochondral fate specification of progenitor cells depended on the expression and activity of miR-199a-5p. Down-regulation of miR-199a-5p was required for terminal osteoblast differentiation while chondrogenic differentiation was severely impaired by its inhibition. miR-199a-5p expression mediated cobblestone-like morphological changes in progenitor cells. Although bone morphogenetic protein-mediated SMAD1/5/9 signaling and expression of downstream osteoblastic transcription factors RUNX2 and Osterix appeared intact in miR-199a-5p expressing cells, miR-199a-5p led to sustained increase in the levels of chondrogenic transcription factor SOX9 and downstream chondrocyte marker genes. Given the importance of miR-199a-5p in dual fate specification of progenitor cells, patients with cis-regulatory variants that increase 199a-5p expression may have reduced osteoblast activity that leads to osteopenia/osteoporosis.

Graphical Abstract

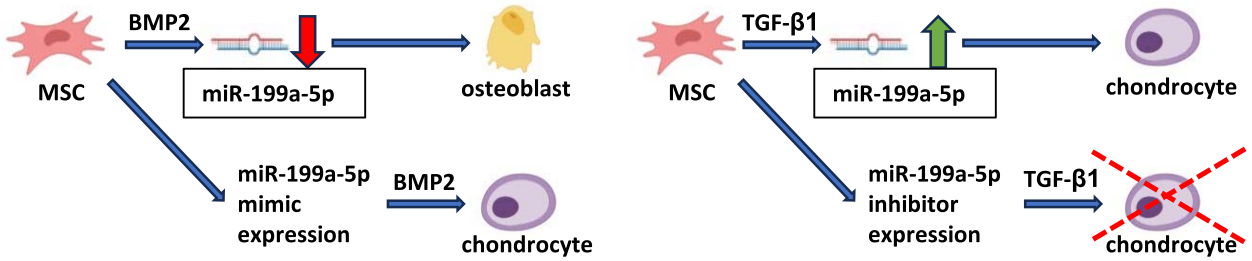

Introduction

Osteoporosis is characterized by decreased bone mineral density (BMD), bone microstructural damage and an increase in bone fragility. It currently affects ~200 million people worldwide [1], and ~43 million people in the United States are at an increased risk for osteoporosis due to low bone mass.[2] Highly heritable genetic traits intensify the environmental, behavioral, and underlying risk factors for osteopenia and osteoporotic fractures. Recent genome wide association studies (GWAS) based on 426 824 subjects have revealed ~518 BMD associated loci (of which 301 are novel).[3] Several upcoming GWAS are now addressing race, ethnicity, and geographic variations to detect rare causal variants which will further increase the numbers of BMD associated loci.

The majority of GWAS variants reported to date resides in non-coding intergenic and intronic regulatory regions[4,5] and in many cases can influence the expression of genes that reside hundreds of kilobases away; thus the nearest gene to a GWAS signal is not necessarily the causal effector gene. The immediate greatest challenge in functionalizing GWAS discoveries is to understand the biological consequences of these regulatory variants on relevant cellular and tissue functions by uncovering the underlying effector gene(s) and defining their molecular roles. Systematic characterization of true GWAS effector genes can significantly improve biological translation by broadening the search for additional drug targets, provide opportunity for drug repositioning studies and precise treatment alternatives.[4]

We recently used functional genomics to discover candidate effector genes residing at DEXA-derived and heel ultrasound-associated BMD GWAS loci by combining assay for transposase-accessible chromatin (ATAC)-sequencing and three-dimensional promoter-focused Capture C based interaction analyses of human mesenchymal stem/progenitor cell (MSC)-derived osteoblasts.[6] This study revealed putative target genes at a total of 46 BMD GWAS loci where some were already known to encode regulators of bone osteogenesis (eg, *SMAD3, SMAD9, SPP1, WLS, FRZB, NOG,* and *MIR31HG)* while others were novel in the context of bone metabolism. Functional follow-up at the "*CPED-WNT16*" and "*STARD3NL*" locus led to the implication of two candidate genes, *ING3* and *EPDR1*. Knock-down of both genes disrupted osteoblastogenesis but enhanced adipogenic differentiation of MSC. Additionally, the functionality of the proxy SNP(s) in regulating *EPDR1* expression during osteoblast differentiation have been validated in hFOB1.19 human fetal osteoblasts by using clustered regularly interspaced short palindromic repeat Cas9 endonuclease (CRISPR-Cas9)-mediated gene editing.[7] These results indicate that our functional genomics approach can powerfully "rule-in" functionally relevant candidate effector genes at BMD GWAS loci and that these effector genes could utilize distinct mechanisms to alter terminal cell fate.

Among several loci where effector genes are yet to be resolved, the heel ultrasound BMD GWAS implicated *DNM3* locus is particularly intriguing given our functional genomic datasets did not implicate any protein coding genes. Instead, the non-coding region harboring four proxy SNPs rs1992549, rs1992550, rs2586393, and rs6694378 in strong linkage disequilibrium with GWAS sentinel SNP rs12041600 contacted the promoter of the long non-coding RNA (lncRNA) *DNM3OS*[6] which serves as a precursor for three microRNA (miR) clusters, *MIR199A2* (encoding miR-199a-5p and miR-199a-3p), *MIR214* (miR-214-5p and miR-214-3p) and *MIR3120* (encoding miR-3120-5p and miR-3120-3p, that are mirror microRNAs complementary to the miR-214[8]). The role of lncRNA *DNM3OS* has been previously studied in the context of murine skeletal development by inserting the *lacZ* gene in the 5'-region to understand its expression pattern and effect of its disruption during development.[9] Since mice embryos homozygous for *lacZ* expression ($Dnm3os^{lacZ/lacZ}$) showed significant downregulation of *Mir199a, Mir199a**, and *Mir214*, this supports *Dnm3os* as the precursor gene for the embedded miRNAs; however, it remains unclear whether *Dnm3os* gene itself or the embedded miRNAs govern the skeletal phenotype. Nonetheless, mice with *Dnm3os* disruption exhibited several skeletal abnormalities after birth, including craniofacial hypoplasia, defects in dorsal neural arches and spinous processes of the vertebrae, and osteopenia. These observations clearly suggest an important role of *DNM3OS* in skeletal homeostasis which is now further supported by our functional genomics dataset that implicates

DNM3OS and *MIR199A2* as candidate effector genes at the *DNM3* locus.

Various studies have shown that the changes in expression levels of miR-199a-5p and miR-199a-3p drive important cellular processes including cell proliferation, migration, and differentiation of endometrial mesenchymal cells, myoblasts, lung fibroblasts and cardiomyocytes by affecting cellular targets such as *VEGFA,* Caveolin-1, *HIF1A,* Sirtuin1, *PGC1A*, and *GATA4*.[10] Aberrant expression of these miRNAs has also been documented in various cancer cells, and their expression patterns tightly relates to invasion, apoptosis, autophagy, and glucose metabolism.[10] The role of these microRNAs has also been examined in context of chondrogenic differentiation of progenitor cells but has produced conflicting reports both in vitro and in vivo. For example, in human articular cartilage, one study showed that the expression of miR-199a-3p is upregulated with age and that *COL2A1*, *ACAN,* and *SOX9* expression were downregulated by expression of miR-199a-3p mimic in human chondrocytes[11]; whereas another study showed downregulation of miR-199a-5p in damaged articular cartilage tissues among osteoarthritis (OA) patients and OA cell culture.[12] Correspondingly, induction of miR-199a-3p has also been demonstrated during chondrogenesis of human adipose-derived stem cells[13] while another study showed that it affected KDM6A/WNT3A signaling to increase adipogenic differentiation of bone marrow-derived MSC.[14] Likewise, murine models have also produced conflicting results with regards to miR-199. miR-199a-3p levels initially decreased but significantly increased at later time points during the course of BMP2-triggered chondrogenesis of a micro-mass culture of C3H10T1/2 cells.[15] In this study, Smad1 was computationally predicted as a putative target of miR-199a-3p and negatively affected the Smad1/Smad4-mediated transactivation of target genes. However, anti-miR-199a-3p was shown to increase the expression of type II collagen, *COMP,* and *SOX9*. MSC isolated from ovariectomized rats increased expression of miR-199a-3p and correlated with decreased osteogenic differentiation due to a downregulation of *Kdm3a*.[16] Rats showed an increased expression of miR-199a-5p in OA tissues and inhibiting its activity favored the survival of chondrocytes, reduced apoptosis and decreased the content of pro-inflammatory cytokines via MAPK4 regulation.[17] Although these studies provide relevance of miR-199a in chondrogenesis across human and murine models, the role of mir-199a-5p during specification of human mesenchymal stem/progenitor cell fate remains elusive.

In this study, we evaluated the BMD GWAS locus *DNM3* in human MSC, where proxy variants rs1992549, rs1992550, rs2586393, and rs6694387 of the GWAS sentinel SNP rs12041600 contact the putative promoters of candidate effector genes *DNM3OS* and *MIR199A2*. Through temporal expression profiling and gain/loss of function studies, we establish that oscillating miR-199a-5p levels regulate terminal fate specification of human MSC into osteoblasts or chondrocytes.

Materials and methods

Culture and treatment of human mesenchymal stem cells

Primary bone-marrow derived human mesenchymal stem cells (hMSC) derived from healthy donors (age range 22 to 29 years) were obtained as individual frozen vials from the Institute of Regenerative Medicine, Texas A&M University. These cells were pre-characterized for cell surface expression (CD166+ CD90+ CD105+ CD36- CD34- CD10- CD11b- CD45-) and tri-lineage differentiation (osteoblastic, adipogenic, and chondrogenic) potential. The generation of the assay for transposase accessible chromatin (ATAC)-sequencing libraries, promoter-focused Capture-C libraries, RNA-sequencing and implication of proxy SNP variants interacting with gene promoters have been previously described.[6] The same set of donor cells were used for osteoblastic characterization in this study. Cells were cultured at a density of 3000 cells/cm^2 using alpha-MEM supplemented with 16.5% FBS (Atlas Biologicals, CO) in standard culture conditions for propagation and used within passage 7. Osteoblast differentiation was achieved using bone morphogenetic protein (BMP) stimulation by adding 200 ng/mL of recombinant human/mouse/rat BMP-2 (R&D Systems, MN) to the cell monolayer expressing miR-199a-5p-mimic, miR-199a-5p-inhibitor or both using osteopermissive media (serum free alpha-MEM additionally supplemented with 25 μg/mL L-ascorbic acid phosphate magnesium salt n-hydrate (FUJIFILM Wako Chemicals USA Corp., VA), 5 mM β-glycerophosphate disodium salt hydrate (Sigma, MO) and 1× insulin–transferrin–selenous acid premix (Corning, NY))[6,18] as described previously. Stimulated cells were harvested at various time points for histochemical alkaline phosphatase staining, RNA extraction, total cell lysate preparation and detection of extracellular calcium as required. Digital quantification of staining levels was performed as described previously.[6]

Chondrogenic differentiation of hMSC

Chondrogenic differentiation was performed using the pellet culture method[19] using high glucose DMEM supplemented with 1% ITS, 25 μg/mL AA2P, 10 μM Dexamethasone, 10 ng/mL TGF-β1 and 4 μg/mL L-proline. Briefly, cells were collected by trypsinization and resuspended at a density of 2.5×10^5 cells in 200 μL chondrogenic differentiation media and plated onto U-bottom 96-wells. Cells were centrifuged at 500 g to form pellets. Media-exchange on the pellets was performed every 3-days by demi-depletion and lasted for a total of 3 weeks as required for each experiment. For total RNA harvest, 3–4 pellets for each donor/each condition was pooled and flash frozen in liquid nitrogen. Pellets were crushed using a pestle fitting a microcentrifuge tube and total RNA was harvested using Trizol using standard procedure. At the end of 3 weeks, pellets were also combined to evaluate Alcian blue staining, DNA content and sGAG expression. For monolayer chondrogenesis, sub-confluent cell monolayers were washed with warm PBS and supplemented with chondrogenic media as above. Media exchange for monolayer chondrogenic culture was performed twice a week at an interval of 3–4 days for a maximum of 2 weeks.

Transfection of hMSCs

Transfection reagents were obtained from Dharmacon Inc. (Lafayette, CO), and detailed information is provided in the Supplementary Information. One day before siRNA transfection, 60 000 hMSCs were seeded onto each well of a 12-well plate using hMSC maintenance media and the next day transfected using DharmaFECT1 transfection reagent (Dharmacon Inc.) following manufacturer's instructions. Two days after the transfection, cells were stimulated with osteogenic or

chondrogenic media. For 3-D chondrogenesis, transfections were carried out in larger culture formats by scaling up the cells and reagent proportionally. Chondrogenic pellets were prepared using 2.5×10^5 transfected cells and propagated for a total of 21 days using differentiation media as described previously. Immobilization of Jagged1 on to culture dishes and subsequent osteoblast differentiation assay using transfected cells were carried out as described previously.[18]

Alcian blue staining

Alcian Blue Staining was performed using chondrogenic pellets after 21 days in culture. Harvested pellets were washed twice with cold PBS and fixed in 10% neutral buffered formalin for 30 minutes. After rinsing off the formalin, the pellets were washed with 70% ethanol, embedded in paraffin and 7 μm sections were prepared. The sections were stained using 3% Alcian blue dye (Poly Scientific) after routine deparaffinization and rehydration protocols. Finally, the sections were counterstained with nuclear Fast Red (EMS), mounted and evaluated under microscope.

DNA content and sGAG determination on chondrogenic pellets

Samples were digested in papain buffer made of EDTA and sodium phosphate, overnight at 65°C. The dimethyl methylene blue assay was used to quantify sGAG concentrations as previously described.[19] sGAG concentrations were normalized to DNA content measured using the PicoGreen DNA assay kit (Thermo Fisher).

Quantitative RT-PCR analysis

A total of 600 ng of total RNA was reverse transcribed using High-Capacity cDNA Reverse Transcription Kit (Applied Biosystems) in a 20 μL reaction. The resulting cDNA was diluted five times, and one microliter cDNA was amplified in a total PCR volume of 10 μL using Power SYBR® Green PCR Master Mix (Applied Biosystems) and gene-specific primers in a QuantStudio Pro 6 (Applied Biosystems) following manufacturer's recommendations. The sequences of primers are provided in the Supplementary Information. Relative expression for each gene was normalized against GAPDH and expressed as fold change over control. Data from at least three different donor lines were combined and reported as mean ± standard deviation.

Mature miR-199a-5p detection was carried out using a miRNA cDNA synthesis kit (abm® Catalog #: G898) as described by the manufacturer with minor modifications. Briefly, 600 ng of total RNA was used for Poly A tailing in a reaction volume of 20 μL. Half of the resulting Poly A tailed RNA was used to generate miRNA cDNA using miRNA Oligo (dT) adapter and OneScript® reverse transcriptase in another reaction volume of 20 μL. Finally, miRNA cDNA was used to quantify the expression level of miR-199a-5p specific forward primer (abm® Catalog #: MPH01240) and a universal 3'- primer (abm® Catalog #: MPH00000) using Power SYBR® Green PCR Master Mix as described above. SNORD48 specific forward primer (abm® Catalog #: MPH00005) was used as house-keeping control.

Immunoblotting

Total cell lysates were prepared for immunoblot analysis as previously described.[18] Briefly, 10–20 μg of protein were loaded into 8%–12% SDS-polyacrylamide gels and electro-transferred onto polyvinyl difluoride membranes. Membranes were blocked for 1 h in 2.5% non-fat skim milk in T-TBS (Tris-buffered saline containing 0.01% Tween-20), and incubated with primary antibodies (see Supplementary Information for antibody information) overnight at 4°C. On the following day, membranes were extensively washed with T-TBS and incubated with horse-radish-peroxidase conjugated secondary antibodies for 1 h at room temperature. Finally, the blots were incubated for 5 min in Supersignal™ West Femto Chemiluminescent Substrate (Fisher Scientific) and data were captured on Bio-Rad Chemi Doc system using appropriate settings for each antibody. Relative band intensities from each blot were calculated using Image Lab software v6 (Bio-Rad) and data from three to four different independent blots were combined for statistical analysis.

Statistical analysis

Data were quantified to express as numerical values for each assay and reported as mean ± SD. Each colored dot represents data obtained from a unique donor. The number of unique donors and assay replicates for each experiment are mentioned in the figure legends. A two-way homoscedastic Student's t-test was performed to determine significance between treatment conditions. The asterisk represents significant difference ($P \leq .05$) compared with control, and "#" represents significant difference between experimental groups ($P \leq .05$). For multiple comparisons, one way ANOVA with Tukey's post hoc test was used after confirmation of normality and equal variance assumptions.

Results

DNM3OS and *MIR199A2* expression decreases during human osteoblast differentiation

We previously reported for the heel ultrasound implicated *DNM3* locus on chromosome 1 that four proxy SNPs rs1992549, rs1992550, rs2586393, and rs6694387 in high linkage disequilibrium with the GWAS sentinel SNP rs12041600 had consistent contact with the promoters of *DNM3OS* and *MIR199A2* in differentiating human osteoblasts derived by BMP2 stimulation of bone-marrow derived human mesenchymal stem/progenitor cells (Figure 1A). These implicated genes are of particular interest given they do not code for proteins: *DNM3OS* is a long non-coding RNA (lncRNA) that also harbors the *MIR199A2* gene, and *MIR199A2* gives rise to two mature microRNAs: miR-199a-5p and miR-199a-3p through an intermediary primary-miRNA transcript pri-miR-199a (Figure 1B).

lncRNA interact with DNA, RNA, and proteins to modulate chromatin function, alter the stability and translation of cytoplasmic mRNAs and interfere with signaling pathways.[20] miRNAs interact with the 3' UTR of target mRNA and directly target up to 60% of protein-coding genes.[21] To understand whether *DNM3OS,* a lncRNA, and *MIR199A2,* a microRNA, are expressed and temporally regulated during osteoblastic differentiation of mesenchymal stem/progenitor cells (MSC), we induced osteoblast differentiation and assessed gene expression. Both *DNM3OS* and pri-miR-199a were detected in unstimulated cells and changed minimally up to 8 h after induction of differentiation (Figure 1C and D). After 24 h, expression levels decreased by ~50%–60% and

A.

GWAS Locus	Sentinel SNP	Proxy SNP (r^2)	Implicated genes (FPKM)	GWAS set
DNM3	**rs12041600**	**rs1992549 (1), rs1992550 (1), rs2586393 (0.99), rs6694384 (0.94)**	***DNM3OS* (8.92)** ***MIR199A2* (NA)**	**Heel**

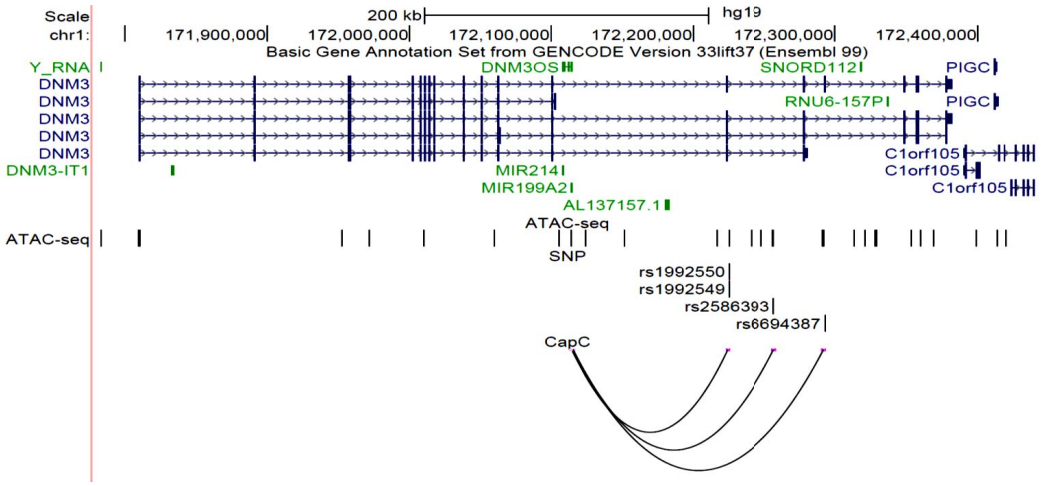

B.

>hsa-mir-199a-2 MI0000281
AGGAAGCUUCUGGAGAUCCUGCUCCGUCGC**CCCAGUGUUCAGACUACCUGUUC**AGGACAAU
GCCGUUGU**ACAGUAGUCUGCACAUUGGUUA**GACUGGGCAAGGGAGAGCA

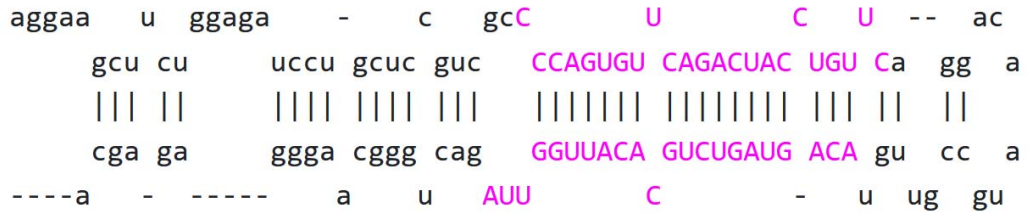

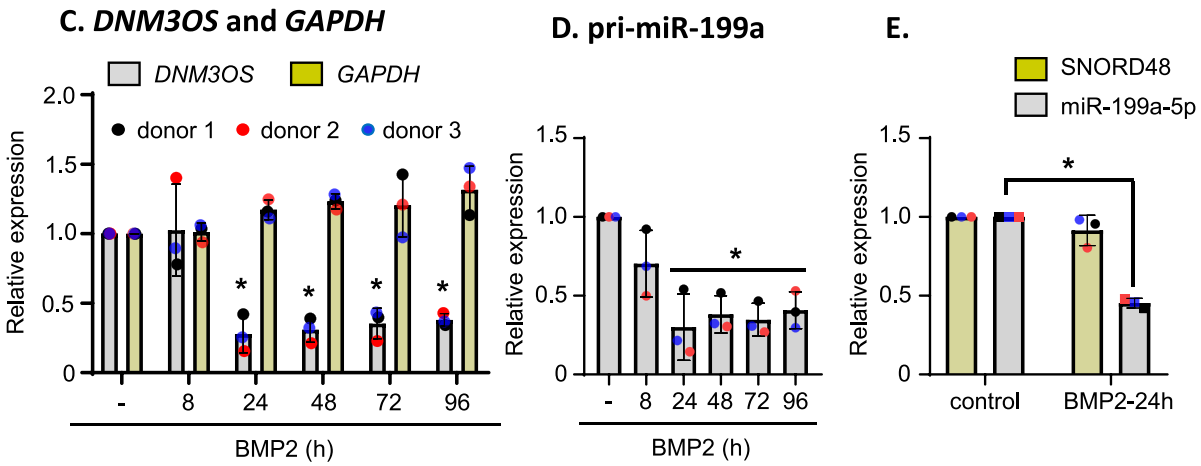

Figure 1. *DNM3OS* and *MIR199A2* expression decreases during human osteoblast differentiation. (A) Top: Four proxy SNP with their degree of correlation (r^2) with the GWAS sentinel SNP rs12041600 at the heel ultrasound BMD locus *DNM3* is shown. Two implicated genes *DNM3OS* and *MIR199A2* alongside with their RNA sequencing reads (FPKM) from differentiating human osteoblasts is also presented. Bottom: UCSC genome browser snapshot of the ATAC-seq and capture-C tracks for the four proxy SNPs contacting the promoter region of the implicated genes. (B) Complete sequence of the human pri-miR-199a-2 with the mature microRNAs miR-199a-5p (red) and miR-199a-3p (blue) is shown. Bottom panel: Predicted secondary structure of pri-miR-199a-2 hairpin is shown. (C, D). Quantitative gene expression levels of *DNM3OS* and *GAPDH* (C) and pri-miR-199a (D) was determined in cells stimulated with 200 ng/mL BMP2 for up to 96 h as indicated. E. The expression level of mature hsa-miR-199a-5p was determined in cells stimulated with BMP2 for 24 h. The level of SNORD48 was evaluated as internal control. Beige columns = SNORD48, grey columns = hsa-miR-199a-5p. Quantitative gene expression data were combined from three independent MSC donor lines (indicated by colored dots) and represented as mean ± SD. $^*P < .05$ comparing no treatment to BMP2 treatment using two-way homoscedastic Student's *t*-tests.

remained steady for 96 h whereas the levels of *GAPDH* (used as house-keeping gene) remained stable (Figure 1C). To correlate that these results are indicative of a decrease in mature miR-199a-5p, we directly measured its levels and an unrelated miRNA, SNORD48, after 24 h of induction of differentiation representing a timepoint of diminished *DNM3OS* and pri-miR-199a expression and the terminal osteoblast commitment phase of MSC where BMP/SMAD signals integrate on to Notch processing and start to accumulate *ALPL, RUNX2* and *SP7*.[18] Mature miR-199a-5p was readily detectable in unstimulated cells and showed ~50% reduction in osteoblast committed cells (Figure 1E), comparable to the observed *DNM3OS* and pri-miR-199a decrease. On the other hand, SNORD48 levels remained comparable up to 24 h suggesting that decreases in *DNM3OS* and miR-199a-5p levels occur specifically during hMSC osteoblast differentiation.

miR-199a-5p-mimic overexpression but not *DNM3OS* knock-down results in morphological changes and impairs terminal osteoblast differentiation

Since decreased expression levels of *DNM3OS* and miR-199a-5p overlapped with the osteoblast commitment phase in MSC,[18] we next evaluated their functional relevance via *DNM3OS* knock-down and miR-199a-5p-mimic over-expression to emulate loss and gain of function during osteoblast differentiation. *DNM3OS* was targeted using a set of four small interfering RNA (siRNA) and the gene-silenced cells were induced to differentiate into osteoblasts. Histochemical evaluation for alkaline phosphatase (ALP) expression (Figure 2A, upper image and lower quantification) and extracellular calcium deposition (Figure 2B, upper image and lower quantification) did not show differences in *DNM3OS*-targeted cells. Analysis of knock-down demonstrated ~60% lower *DNM3OS* levels in *DNM3OS* siRNA-treated cells (Figure 2C). In non-targeting siRNA transfected cells, the levels of *DNM3OS* decreased upon BMP2 stimulation, but BMP2 did not further decrease *DNM3OS* levels in the *DNM3OS* siRNA group (Figure 2C). Additionally, *DNM3OS* knock-down did not affect gene expression patterns of BMP/SMAD signal transduction-relevant genes (*ID1, ALPL, RUNX2*, and *SP7*) (Figure S1).

Contrary to the cells transfected with *DNM3OS* siRNA, cells transfected with miR-199a-5p-mimic revealed an increase in ALP staining (Figure 2D, upper image and lower quantification) but surprisingly, completely inhibited calcium deposition into the extracellular matrix (ECM) as determined by Alizarin red S staining (Figure 2E, upper image and lower quantification) after BMP2 stimulation. During the same duration, control cells had already deposited significant amount of calcium into the ECM even though ALP staining levels were lower compared to miR-199a-5p-mimic transfected cells. Although, the true effect on cell proliferation after miR-199a-5p expression cannot be effectively captured in our osteoblast differentiation assay due to serum-free conditions and the use of sub-confluent cultures to link increased ALP staining and absence of calcium deposition, the cell numbers were comparable up to 4 days in presence or absence of BMP2 (data not shown and see below). Remarkably, the miR-199a-5p-mimic induced a profound morphological change in treated cells by 5 days after transfection, demonstrating a cobble-stone like morphology consistent with articular chondrocytes in monolayer culture,[22] compared to a clear fibroblastic morphology in control cells (Figure 2F).

Morphological changes and inhibition of extracellular calcium deposition are restored when cells treated with miR-199a-5p mimic are also treated with an inhibitor

Given that increased ALP expression and morphological change were prominent features of miR-199a-5p-mimic over-expression, we next evaluated the specificity of its effect by co-introducing miR-199a-5p-inhibitor. Equimolar concentrations of miR-199a-5p-mimic, miR-199a-5p-inhibitor or both were introduced into MSC, and the cells were stimulated with or without BMP2. BMP2 stimulation led to an increase in histochemical ALP staining in miR-199a-5p-mimic expressing cells but staining returned to the levels of controls cells in cells co-expressing both miR-199a-5p-mimic and inhibitor (Figure 3A and B). This change was specific for BMP2 stimulated conditions as basal ALP staining levels did not change. There was no effect of miR-199a-5p-inhibitor alone, compared to control cells under stimulated conditions. Cell numbers did not change under unstimulated conditions but decreased slightly in cells expressing miR-199a-5p-inhibitor stimulated with BMP2 after 4 days (Figure S2). Morphological changes were again apparent, and cells expressing miR-199a-5p-mimic showed a flatter, cobblestone like morphology, which reverted back to typical control morphology of slender spindle-shaped fibroblastic appearance with miR-199a-5p-inhibitor treatment both in presence and absence of BMP2. These results suggested that the changes in morphology are specific effects of miR-199a-5p-mimic and can be counteracted by co-introducing miR-199a-5p-inhibitor.

The resolution of morphological differences by co-expression of miR-199a-5p-inhibitor in miR-199a-5p-mimic expressing cells prompted us to evaluate effect on terminal osteoblast differentiation. We observed a clear absence of calcium deposition by miR-199a-5p-mimic expressing cells in presence of BMP2, which was reversed by co-treatment with miR-199a-5p-inhibitor (Figure S3D and E). As observed with minimal differences in morphological features, cells expressing only miR-199a-5p-inhibitor deposited comparable levels of calcium into the ECM after BMP2 stimulation. These results clearly establish that continued miR-199a-5p activity blunts terminal osteoblast differentiation and possibly reprograms the cells to an alternative cellular fate.

miR-199a-5p-mimic expression leads to sustained SOX9 expression and induction of chondrogenic genes after BMP2 stimulation

The lack of terminal osteoblast differentiation (Figures 2E and 3D) and morphological features reminiscent of monolayer chondrocytes[22] in miR-199a-5p-mimic expressing cells (Figure 2F and 3C) were further investigated with regards to changes in BMP/SMAD signaling and downstream signal propagation. The phosphorylation of SMAD1/5/9 levels did not significantly differ in cells expressing miR-199a-5p-mimic (Figure 4A) suggesting that BMP-receptor expression is comparable and miR-199a-5p-mimic expressing cells transmit equivalent initial down-stream BMP signals for osteoblast

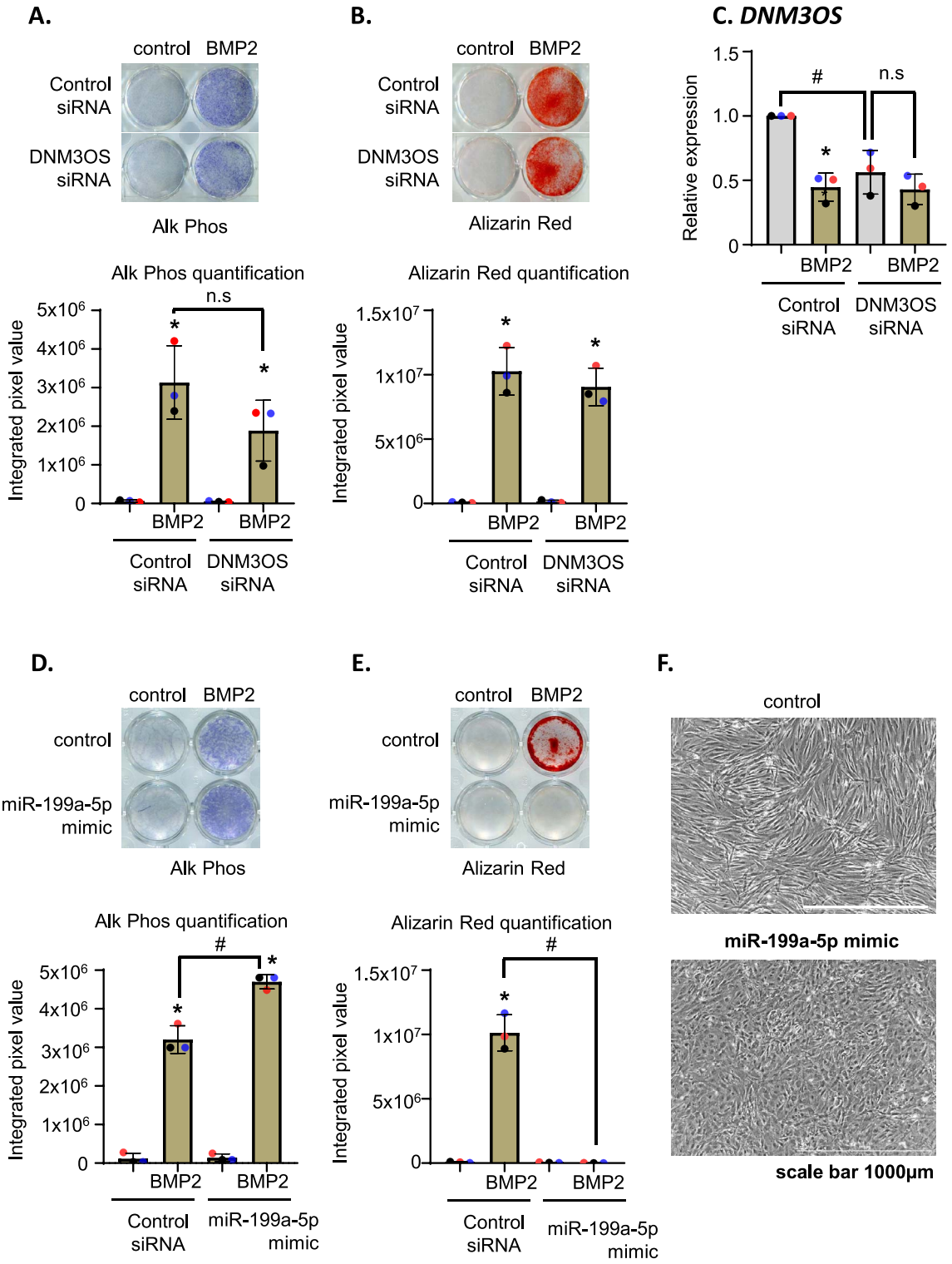

Figure 2. Over-expression of miR-199a-5p-mimic in hMSC results in morphological changes and impairs extracellular calcium deposition, but enhances alkaline phosphatase. (A) DNM3OS siRNA transfected hMSC were stimulated with or without BMP2 (200 ng/mL) for 4 days and alkaline phosphatase expression was histochemically determined (a representative stained plate image upper panel and lower histogram depicting quantification of data from three unique donor lines). (B) Extracellular calcium deposition was evaluated by alizarin red S staining of DNM3OS siRNA transfected cells stimulated with or without BMP2 for 10 days and presented as in (A). (C) Quantitative gene expression analysis to determine relative expression levels of *DNM3OS* from three independent hMSC donor lines after DNM3OS silencing. Gray columns = No BMP; dark beige columns = BMP treatment for 3 days. Columns = means, error bars = SD. $^{*}P < .05$ comparing No treatment to BMP2 treatment, $^{\#}P < .05$ comparing control siRNA to DNM3OS siRNA (two-way homoscedastic Student's *t* tests), n.s = not significant. (D, E). miR-199a-5p-mimic transfected hMSC were stimulated with or without BMP2 as above. Alkaline phosphatase expression (D) and extracellular calcium deposition (E) was histochemically determined after 4 days and 10 days respectively and presented as in (A). (F) Phase contrast images of control or miR-199a-5p-mimic transfected cells after culturing for 3 days in serum-free ostepermissive media. 3×3 images were captured using 10× objective of Lionheart automated microscope and stitched. Scale bar = 1000 μm. A representative result among three independent donor lines is shown.

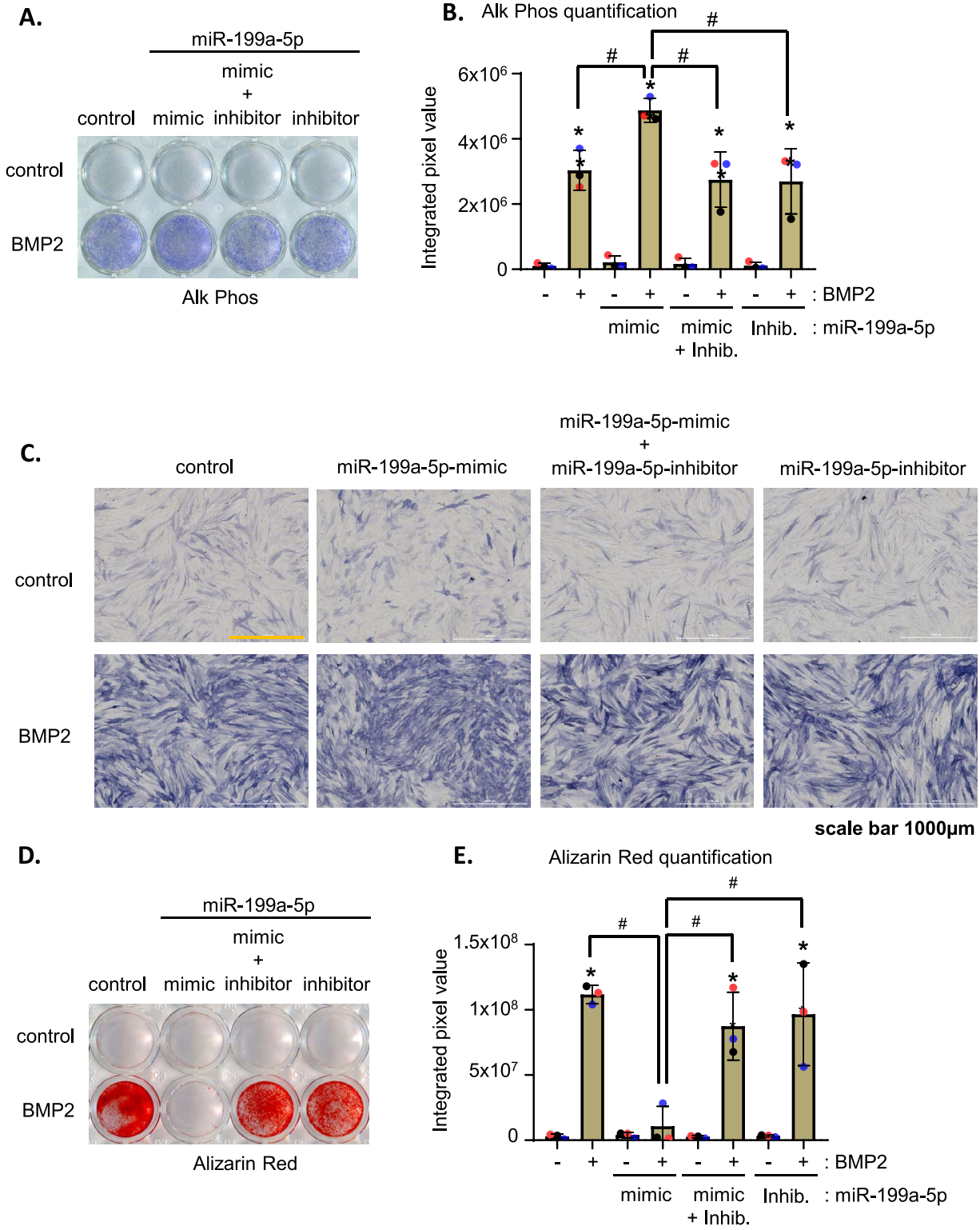

Figure 3. Morphological changes and inhibition of extracellular calcium deposition are restored when cells treated with miR-199a-5p-mimic are also treated with an inhibitor. (A) hMSC were transfected with equimolar concentrations of miR-199a-5p-mimic, miR-199a-5p-inhibitor, or both for 2 days and transferred to osteopermissive media with or without BMP2 stimulation for 4 days. At the end of the treatment period, alkaline phosphatase expression was histochemically determined. A representative result among three unique donors is shown. (B) Quantitative image analysis of stained plates from three independent donor lines were performed and integrated pixel values were compared within transfection and stimulation conditions. (C) Color brightfield images of the alkaline phosphatase-stained wells from (A) is presented. Each image represents 3×3 stitched images taken using 10× objective of Lionheart automated microscope. Scale bar = 1000 μm. (D) Cells stimulated as in (A) were continued in culture for a total of 10 days. Calcium deposition into the extracellular matrix was evaluated by alizarin red staining. E. Alizarin red levels were digitally quantified and expressed as integrated pixel values as in (B). Data from three independent donor lines were combined for the analysis. Gray columns = No BMP; dark beige columns = BMP treatment. Columns = means, error bars = SD. $^{*}P < .05$ comparing No treatment to BMP2 treatment, $^{\#}P < .05$ comparing miR-199a-5p-mimic vs control or miR-199-5p-mimic plus miR-199a-5p-inhibitor (one way ANOVA with Tukey's post hoc test).

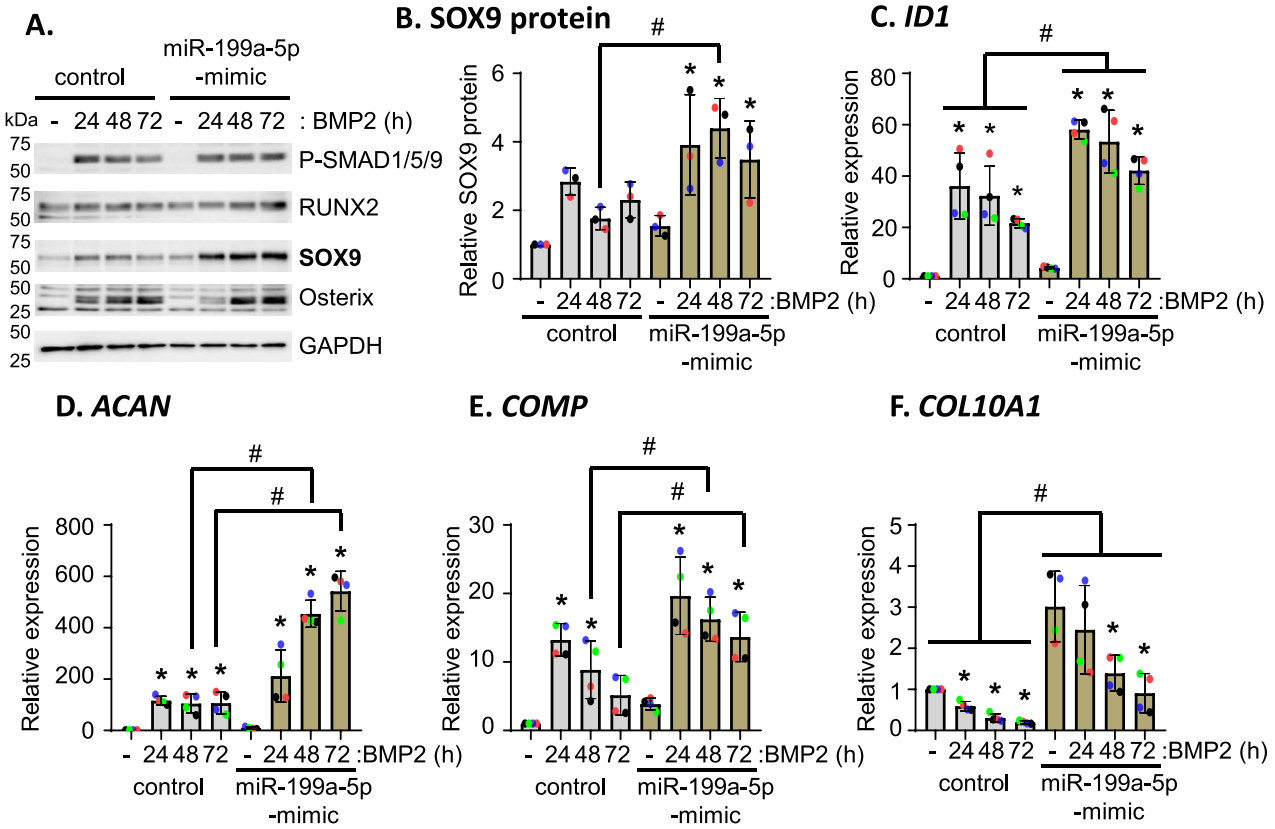

Figure 4. miR-199a-5p-mimic over-expression leads to sustained SOX9 expression and induction of chondrogenic genes after BMP2 stimulation. (A) hMSC were transfected with non-targeting control or miR-199a-5p-mimic for 2 days and transferred to osteopermissive media with or without BMP2 stimulation as indicated for up to 72 h. At the end of the treatment period, total cell lysate was prepared and immunoblotted to determine protein levels of phosphorylated SMAD1/5/9, RUNX2, SOX9, Osterix, and GAPDH. (B) Quantitative densitometric analysis of SOX9 protein expression from three independent donor lines were performed after normalizing against GAPDH and presented as relative change compared to each donor control. SOX9 levels from non-stimulated control cells is arbitrarily set to 1 and expressed as fold change for transfection and stimulated conditions. C-F. Cells were transfected as in (A) and total RNA was used to determine gene expression analysis of (C) *ID1*, (D) *ACAN*, (E) *COMP*, and (F) *COL10A1*. Gray columns = control transfection group; dark beige columns = miR-199a-5p-mimic transfection group. Columns = means, error bars = SD from four independent donor lines $^{*}P < .05$ comparing No treatment to BMP2 treatment, $^{\#}P < .05$ comparing control vs miR-199a-5p-mimic using one way ANOVA with Tukey's post-hoc test.

differentiation. The expression of the canonical BMP/SMAD target gene *ID1* (Figure 4C) also supported this notion as its level did not decrease but instead showed higher levels after BMP2 stimulation in the presence of miR-199a-5p-mimic. Further, protein levels of RUNX2 and Osterix in miR-199a-5p-mimic expressing cells were either comparable to control cells or slightly enhanced after 48 h of BMP2-stimulation which was also reflected at the mRNA level (Figure 4A, Figure S3A, and data not shown). This was particularly intriguing because despite proper expression of osteoblastic transcription factors and alkaline phosphatase, the absence of calcium deposition into the ECM could not be explained. Considering the chondrocytic appearance after miR-199a-5p-mimic expression, we evaluated whether SOX9, a master chondrogenic transcription factor could be involved. As shown in Figure 4A (immunoblot panel) and Figure 4B (quantification), in the control group, a minor increase of SOX9 protein was observed after 24 h of BMP2 stimulation that gradually returned towards baseline levels within 72 h (Figure 4B). In miR-199a-5p-mimic expressing cells, however, robust induction of SOX9 protein was observed after 24 h of BMP2 stimulation that remained elevated until 48 h, at which point the SOX9 protein levels were significantly higher than control cells.

Elevated and sustained expression of SOX9 upon BMP2 stimulation of miR-199a-5p-mimic expressing cells suggested that cell fate was biased towards chondrocytes, and we next evaluated expression levels of *ACAN*, *COMP*, *COL10A1*, and *SOX9* as markers of chondrocytes. miR-199a-5p-mimic expressing cells exhibited elevated level of these genes under unstimulated conditions (Figure 4D-F and data not shown), and *ACAN* dramatically increased with BMP2 stimulation (Figure 4D). *COMP* expression increased after 24 h of BMP2 stimulation in both groups but started to decline afterwards, with a slower decline noted in miR-199a-5p-mimic expressing cells. By 72 h, miR-199a-5p-mimic expressing cells still expressed about 2-fold more *COMP* than the control cells (Figure 4E). *COL10A1* levels were also significantly higher in miR-199a-5p-mimic group under unstimulated conditions, and BMP2 stimulation led to a reduction of *COL10A1* expression in both groups. Compared to control groups that had lost ~90% of its initial expression, its expression became comparable to the initial levels of the unstimulated cells by 72 h upon miR-199a-5p-mimic expression (Figure 4F). *SOX9* levels followed a similar trend as observed with the protein levels (Figure 4A and B and data not shown). Based on these results, miR-199a-5p expressing cells in 2D culture appear committed for chondrogenic differentiation.

As mentioned previously, the 24 h time point after BMP2 stimulation marks the terminal osteoblast commitment phase of MSC, RUNX2 protein levels are elevated, and Osterix gene transcription levels and protein are increased.[18] This is also the time point when BMP/SMAD signals influence canonical Notch signaling, which is required for terminal differentiation.[18] Intriguingly, direct stimulation of MSC with Notch ligand Jagged1 (JAG1) leads to enhanced ALP expression and calcium deposition in human MSC without increased BMP signaling and without significantly affecting RUNX2 and Osterix levels,[18,23,24] Thus, we evaluated whether JAG1-mediated terminal osteoblast differentiation could by-pass the osteoinhibitory effects of miR-199a-5p-mimic. JAG1 stimulation of miR-199a-5p-mimic expressing cells depicted a modest increase in ALP staining (a result comparable to BMP2 stimulated cells; Figures 2C and 3A), but there was no major differences in extracellular calcium deposition compared to mimic control cells (Figure S4A and B). At the signal propagation level, Notch receptor processing (Figure S4C), the protein levels of Notch signal transducer RBPJ, and osteoblastic transcription factors Osterix and RUNX2 were comparable in JAG1-stimulated cells in the presence of miR-199a-5p-mimic over-expression. The effect of miR-199a-5p-mimic on SOX9 protein during direct JAG1 stimulation was also comparable despite a minor decrease in basal levels of SOX9 protein[18] (Figure S4C, and data not shown). Unlike BMP signaling which increases SOX9, JAG1 actually appears to result in downregulated SOX9. Collectively, these results suggest that the effect of miR-199a-5p-mimic on chondrocyte bias requires elevated Sox9.

miR-199a-5p-inhibition partially restores miR-199a-5p-mimic-dependent SOX9 expression and chondrogenic genes to control levels during osteoblast differentiation

Next, considering the restoration of calcium deposition and reversal of morphological changes induced by miR-199a-5p-mimic in cells co-expressing miR-199a-5p-inhibitor (Figure 3C and D), we examined whether SOX9 protein levels and chondrocyte marker genes also revert towards the control cells. Immunoblot analysis (Figure 5A) and quantification (Figure 5B) shows that the enhanced SOX9 protein levels after BMP2 stimulation of miR-199a-5p-mimic expressing cells decreases when miR-199a-5p-inhibitor is co-expressed. This reduction was also observed at protein and mRNA levels of RUNX2 and Osterix in cells expressing miR-199a-5p-inhibitor under BMP2 stimulated conditions (Figure 3A and Figure SB, and data not shown). Despite lower RUNX2 and Osterix protein expression in miR-199a-5p-inhibitor expressing cells compared to control or miR-199a-5p-mimic expressing cells, their levels were still modestly higher in the BMP2 stimulated cells over unstimulated cells. This could partly explain the deposition of calcium into the ECM by cells expressing miR-199a-5p-inhibitor because continued accumulation of RUNX2 and Osterix protein occurred over time in contrast to SOX9 protein levels.

The resolution of SOX9 expression towards control cells were examined in terms of canonical BMP/SMAD target gene *ID1* and chondrocytic genes *ACAN, COMP*, *COL10A1,* and *SOX9*. As expected, miR-199a-5p-mimic-dependent increase in expression of these genes (Figure 5C-F and data not shown) reversed towards the levels of the control cells under both non-stimulated and BMP2 stimulated conditions in cells co-expressing the miR-199a-5p-inhibitor. Collectively, these results suggest that while there is transient upregulation of SOX9, eventually the impact of RUNX2 and Osterix activity dominate to achieve hMSC osteoblast fate specification. On the other hand, sustained miR-199a-5p activity creates a favorable situation for enhanced SOX9 expression and despite enhanced RUNX2 and Osterix expression in cells expressing miR-199a-5p-mimic, terminal osteoblast differentiation is blunted.

DNM3OS and pri-miR-199a levels concurrently increase with chondrocyte marker genes during chondrogenic pellet cultures of hMSC

Motivated by the chondrocytic phenotype of cells in presence of miR-199a-5p-mimic, we examined the temporal regulation of the implicated genes *DNM3OS* and *MIR199A2* during 3-D chondrogenesis using pellet culture method using TGF-β1 supplementation as a reliable and robust model of hMSC chondrogenesis.[25] The expression of *DNM3OS* (Figure 6A) followed a biphasic trend with gradual decline over the first three days, but its expression started to increase after the fourth day and remained elevated throughout the 2-week period. Unlike *DNM3OS*, pri-miR-199a expression oscillated at lower levels for the first 3 days (Figure 6B), but its expression levels rose dramatically after the fourth day and continued to increase further which was comparable to *DNM3OS*. The expression of chondrocytic marker genes *SOX9, COL2A1, ACAN, COMP, COL10A1,* and *HAS3* were also evaluated in parallel (Figure 6C-H) and while there appeared to be some variability in their expression during the first 4 days after induction of differentiation, their expression levels consistently increased after the 7th day and concurrently followed *DNM3OS* and pri-miR-199a expression trends. This tight correlation between *DNM3OS,* pri-miR-199a and chondrogenic marker genes expression was evaluated next using miR-199a-5p-mimic or miR-199a-5p-inhibitor.

Inhibition of miR-199a-5p function severely impairs chondrogenesis

Given the tight correlation in expression pattern of chondrogenic genes with pri-miR-199a, we evaluated the changes in chondrogenic differentiation after inhibiting or enhancing miR-199a-5p activity. Cells were transfected with non-targeting control, miR-199a-5p-mimic or miR-199a-5p-inhibitor before chondrogenic hMSC pellet cultures were started. Pellets were harvested after 21 days and evaluated for chondrogenic differentiation using Alcian blue staining and the expression of sGAG. No significant differences on Alcian blue staining were observed between control and miR-199a-5p-mimic expressing cells (Figure 7A) indicating that further increasing miR-199a-5p levels beyond a certain threshold does not appreciably improve hMSC chondrogenesis. However, miR-199a-5p-inhibitor almost completely ablated Alcian blue staining (Figure 7A) and the pellet sizes were also considerably smaller for all the donor lines. The lack of Alcian blue staining was corroborated by sGAG levels, which showed significantly lower levels at days 7–21, whereas no differences in sGAG levels were observed between control and miR-199a-5p-mimic expressing cells (Figure 7B and D). This change in sGAG deposition did not result from impaired

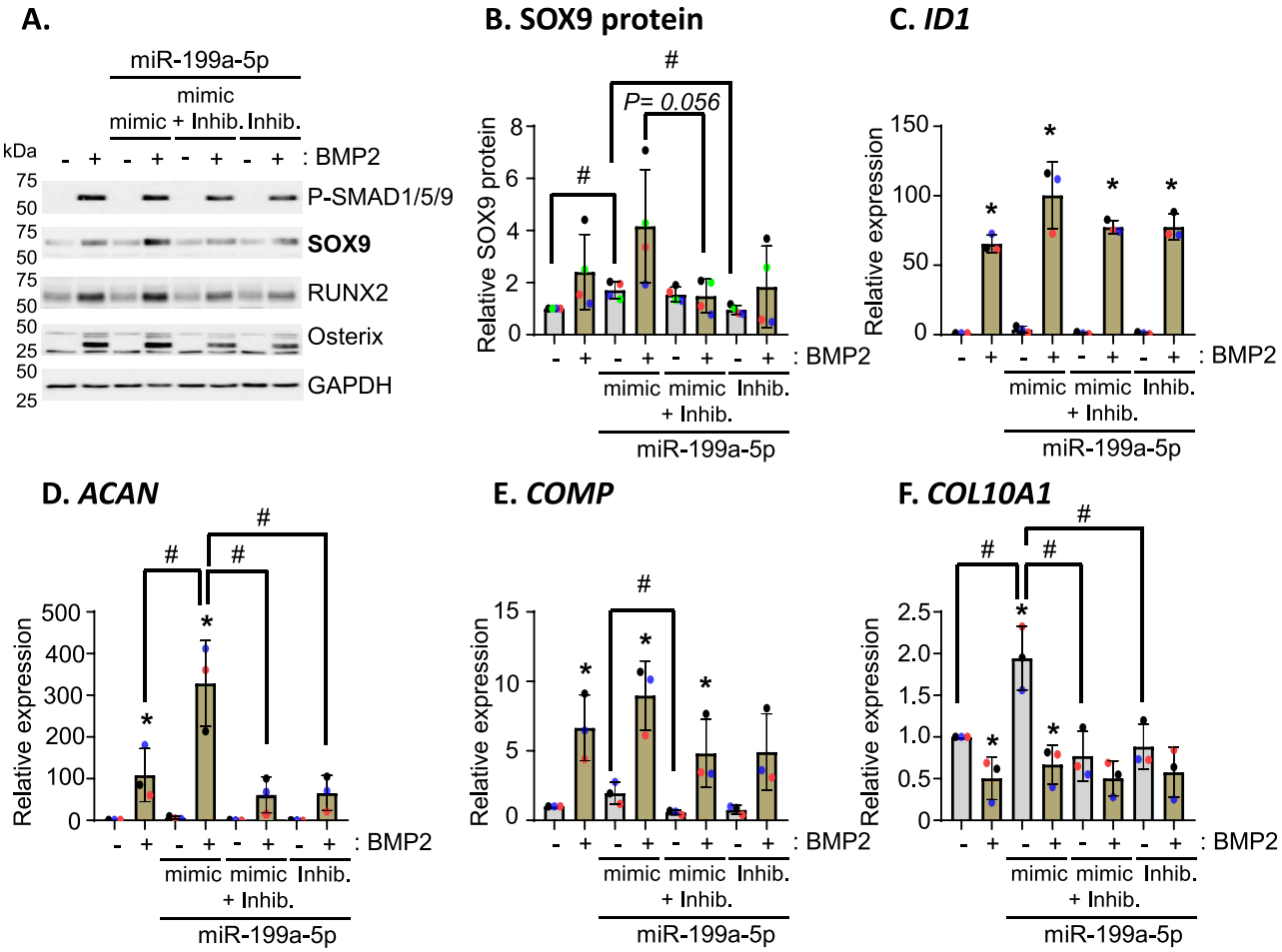

Figure 5. miR-199a-5p-inhibitor co-transfection partially restores the SOX9 expression and associated chondrogenic marker genes to control levels. (A) hMSC were transfected with equimolar concentrations of miR-199a-5p-mimic, miR-199a-5p-inhibitor, or both for 2 days and transferred to osteopermissive media with or without BMP2 stimulation for 3 days. At the end of the treatment period, total cell lysate was prepared and immunoblotted to determine levels of phospho-SMAD1/5/9, SOX9, RUNX2, Osterix, and GAPDH proteins. (B) Quantitative densitometric analysis of SOX9 protein expression from four independent experiments using two unique donor lines is presented as relative change compared to each technical replicate. SOX9 levels were normalized against GAPDH and the expression levels of non-targeted control cells without BMP2 stimulation is arbitrarily set to 1 to calculate fold change for transfection and stimulated conditions. (C-F) Cells were transfected as in (A) and total RNA was used to determine gene expression analysis of (C) *ID1*, (D) *ACAN*, (E) *COMP*, and (F) *COL10A1*. Gray columns = no BMP; dark beige columns = BMP2 stimulation. Columns = means, error bars = SD from three independent donor lines $^{*}P < .05$ comparing No treatment to BMP2 treatment, $^{\#}P < .05$ comparing miR-199a-5p-mimic vs other groups as indicated using two-way homoscedastic Student's *t*-tests.

cell viability as DNA content was comparable across groups at each timepoint (Figure 7C).

Analysis of chondrogenic gene expression further corroborated Alcian blue and sGAG analyses. Whereas control and miR-199a-5p-mimic expressing cells exhibited expected increase in SOX9, *COL2A1*, *ACAN*, *COMP*, and *COL10A1* expression over the 3-week period, miR-199a-5p-inhibitor drastically reduced the expression of these genes throughout the culture duration (Figure 7E-H). Besides *COMP*, which exhibited some time-dependent increase in expression of miR-199a-5p-inhibitor treated cells (Figure 7H), all other genes failed to increase during the experiment. Since there was no significant difference in the DNA content between cells expressing control, miR-199a-5p-mimic or miR-199a-5p-inhibitor at all time durations (Figure 7C), the reduction of chondrogenic marker genes by miR-199a-5p-inhibition cannot be attributed to defective cell proliferation. Counterintuitively, we observed that miR-199a-5p-mimic expressing cells exhibited lower levels of *COL2A1*, *ACAN*, *COMP*, and *COL10A1* at 21 days compared to control cells (Figure 6G-I), which did not appear to influence pellet sGAG content or Alcian blue staining. This result may be attributable to differential chondrogenic kinetics between control and miR-199a-5p-mimic cells. These overall results were further corroborated in monolayer chondrogenesis (Figure S5). Taken together, miR-199a-5p activity favors chondrogenic differentiation of human mesenchymal progenitor cells. Even though we did not observe that increasing miR-199a-5p activity enhanced chondrogenesis, inhibiting its activity severely impairs chondrogenic marker gene expression and chondrogenic differentiation.

Discussion

The terminal fate specification of cells becoming chondrocytes or osteoblasts depends on multiple signaling pathways.[26] Changes in cell shape of chondrocytes temporally manifests an intricate interplay of signals transmitted within the cells to

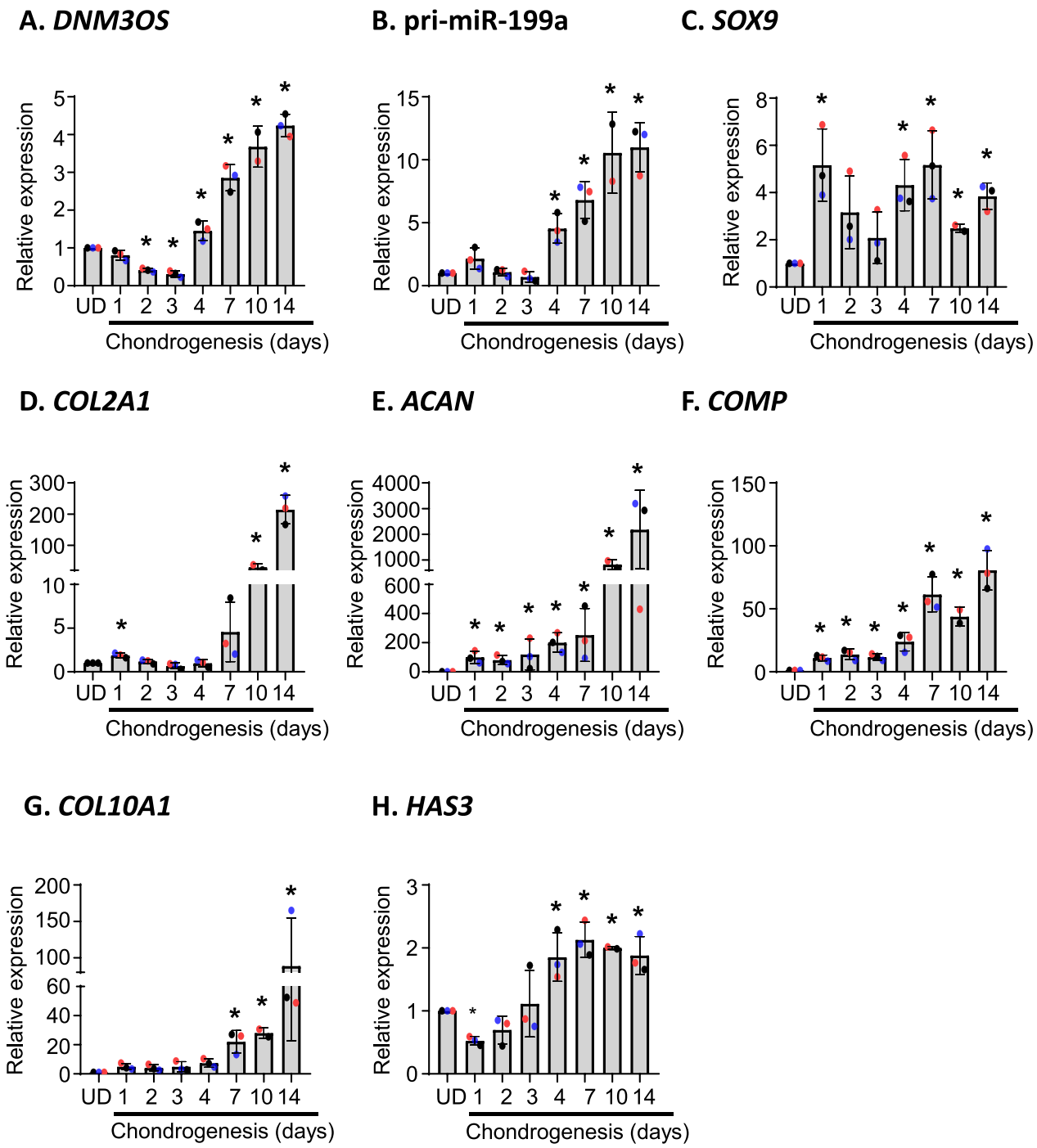

Figure 6. *DNM3OS* and pri-miR-199a levels increases during hMSC chondrogenesis. hMSC was induced to undergo chondrogenesis using pellet culture method and total RNA was harvested at various intervals up to 14 days. Gene expression levels of (A) *DNM3OS,* (B) Pri-miR-199a, (C) *SOX9,* (D) *COL2A1,* (E) *ACAN,* (F) *COMP,* (G) *COL10A1,* and (H) *HAS3* were compared to undifferentiated cells at day 0 (UD). Combined expression levels from three unique hMSC donor line is presented. $^{*}P < .05$ comparing undifferentiated cells to cells at various days of differentiation using two-way homoscedastic Student's *t*-tests.

delicately balance output from osteoblastic and chondrocytic transcription factors[27,28]. Dysregulation of these processes can result in skeletal pathologies and overall changes in bone mineral density. In this study, we present evidence that the miR-199a-5p embedded in the lncRNA *DNM3OS* is a critical regulator of MSC osteochondral fate specification at the BMD GWAS locus *DNM3*. During BMP2-mediated human osteoblastogenesis, the expression of *DNM3OS* and miR-199a-5p decreased with concomitant expression of osteoblastic transcription factors RUNX2 and Osterix.

The expression of *DNM3OS* and miR-199a-5p temporally increased and positively correlated with chondrocyte marker genes during both two-dimensional and three-dimensional chondrogenesis. Oscillating miR-199a-5p activity is functionally relevant for MSC fate specification into osteoblasts and chondrocytes because miR-199a-5p mimic

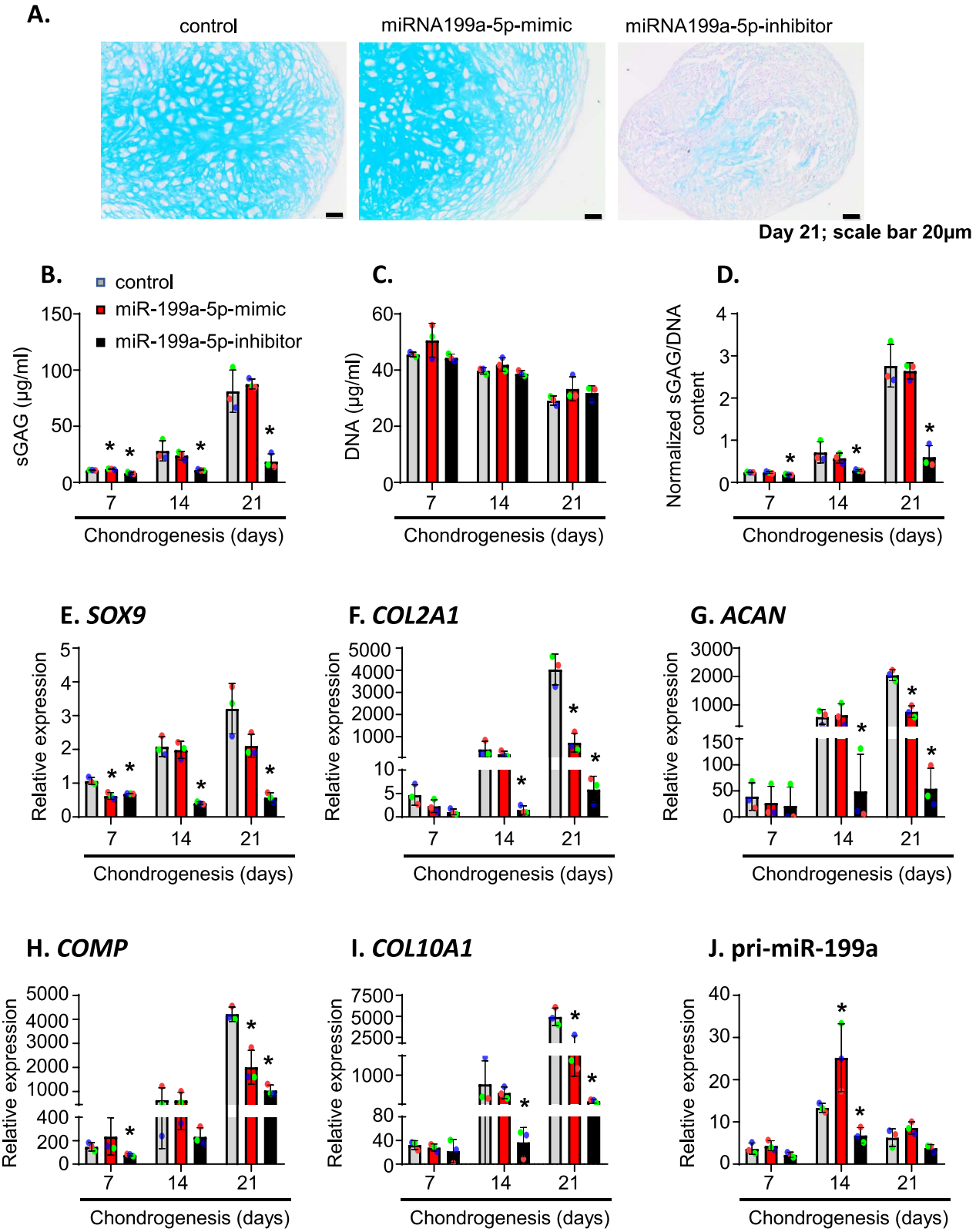

Figure 7. Inhibition of miR-199a-5p activity severely impairs human chondrogenesis. (A) hMSC transfected with non-targeting control, miR-199a-5p-mimic or miR-199a-5p-inhibitor were cultured as pellets using chondrogenic differentiation medium for 21 days. Alcian blue staining was performed to determine the extent of extracellular matrix deposition. (B) Chondrocytic pellets generated from cells transfected as above were harvested at 7-, 14- or 21-days and the levels of sGAG was determined. (C) Total DNA amount in cells cultured as in (B) was evaluated. (D) Normalized sGAG/DNA content within the chondrocyte pellets as above is shown. Alcian blue staining is representative of two independent experiments performed with two hMSC donor lines. The levels of sGAG and DNA were evaluated using three independent hMSC donor lines by combining multiple pellets for each unique donor line. Total RNA from chondrogenic cell pellets as above was harvested and gene expression levels of (E) *SOX9,* (F) *COL2A1,* (G) *ACAN,* (H) *COMP,* (I) *COL10A1,* and (J) Pri-miR-199a were determined relative to undifferentiated cell. Combined expression levels from three unique hMSC donor line are presented. $^{*}P < .05$ compared to control pellets using two-way homoscedastic Student's *t*-tests.

expression disrupted terminal osteoblast maturation by favoring chondrogenesis while direct inhibition of miR-199a-5p activity results in decreased chondrogenic pellet size, extracellular matrix accumulation and downmodulated chondrocyte marker gene expression. miR-199a-5p overexpression accompanied a marked change in overall MSC morphology, and osteogenic BMP2 stimulation led to a sustained expression of chondrogenic transcription factor SOX9 and chondrocyte marker genes – all of which were reversed upon miR-199a-5p inhibition. These results clearly establish miR-199a-5p as an effector gene at the osteoporosis GWAS locus *DNM3* and highlight the possible role of GWAS proxy SNPs in its contextual regulation of BMD accrual.

GWAS is only a first step in uncovering loci contributing to particular phenotypic differences that pinpoint sets of single nucleotide polymorphisms (SNP) in linkage disequilibrium with the sentinel SNP[29] (SNPs that are frequently co-inherited in a population). The resulting regions of associations vary in size and typically implicate multiple genes, only a subset of which is causal in relevant cells and tissues. Often GWAS identified SNPs reside in non-coding regions and function by altering gene regulation through changes in transcription factor binding sites, the 3-dimensional structure of the genome, or alternative splicing. Thus, the challenge of GWAS lies in identifying the actual causal effector gene(s) and understanding the mechanisms by which these genes influence the pathogeneis of the given phenotype. Furthermore, for a complex trait such as BMD, GWAS implicated genes do not necessarily represent central hub genes but rather may indirectly regulate multiple processes in functionally relevant cells and tissues. Examples of this are the BMD GWAS effector genes *EPDR1, ING3,* and *PRPF38A,* knockdown of which resulted in disrupted osteoblastogenesis but favored hMSC adipognensis.[6,7,30] miR-199a-5p embedded within the lncRNA *DNM3OS*, however, represents as a modulator of chondrocytic hub gene *SOX9* regulation, which it achieves via contextual changes in expression levels to specify chondrogenic or osteoblastic fate of MSC in response to specific intracellular differentiation signals.

Although, bona fide mRNA targets of miR-199a-5p remain to be determined, our data clearly indicates that miR-199a-5p activity enhances SOX9 expression and presumably functions by reducing the expression of SOX9 transcriptional repressors. Since the SOX9 gene is regulated at numerous levels, including activity of multiple enhancers, methylation of the promoter, and various histone modifications,[31] it is possible that the miR-199a-5p effects on SOX9 gene regulation could encompass changes in cis-regulatory elements and epigenetic regulation at multiple levels. Additionally, SOX9 expression is known to be positively co-related with the activation of Hedgehog,[32] BMP signaling,[33] fibroblast growth factor signaling, hypoxia and mechanical loading[34] and inhibited after the activation of Notch and canonical WNT signaling pathways.[35] Specifically, changes in extracellular matrix organization are known to affect integrins and the mechanical properties of the cells leading to osteoblastic or chondrogenic differentiation. For example, $\alpha 2\beta 1$ signaling is required for osteoblast differentiation[36] and Integrin $\beta 1$ has been shown to play a role in chondrogenic differentiation.[37] Moreover, MSC cultured on lower stiffness substrates are known to show elevated expression of *ACAN*, *SOX9*, and *COL2* and proteoglycan content.[38] The implications of miR-199a-5p on these signal transduction modules and extracellular matrix assembly could also be functionally relevant and needs to be addressed in future studies because miR-199a-5p expression induced morphological change in hMSC.

Despite being a critical regulator of human osteoblast differentiation,[18] Notch signaling, does not seem to be involved in mineralization defect of cells over-expressing miR-199a-5p because BMP-2 mediated expression of canonical Notch ligand JAG1 and Notch processing remained intact in the presence of miR-199 mimic (data not shown). Additionally, Jag1 stimulation of miR-199a-5p mimic expressing cells did not increase SOX9 expression (and in fact Jag1 appears to decrease SOX9) and depicted comparable levels of calcium into the extracellular matrix relative to control cells (Figure S4). These results suggest that miR-199a-5p does not intersect with Notch signaling.

In silico bioinformatics prediction using multiple databases indicates an overlap of 79 putative target genes of miR-199a-5p (Table S1) and 61 putative target genes of miR-199a-3p (Table S2). Functionally miR-199a-5p target genes are implicated in various biological processes such as regulation of signal transduction, epithelial to mesenchymal transition, non-canonical Wnt signaling pathway, ear development etc. (Figure S6A). Notable target genes include 11 transcriptional regulators (eg, *MYRF, ZBTB42, SNAI1, ONECUT2, ZNF704, PAX3, RFX3, CLOCK, NPAS2, ETS1, ZNF516*), signaling molecules (*TGFB2*, *ACVR2B*, *DDR1*, *PLXNA2*, *GPR63* etc.), and genes affecting extracellular matrix and bone specification pathways (*FZD4*, *FZD6*) (Figure S6B). With regards to transcriptional regulators as putative targets of miR-199a-5p, *SNAI1* could be of particular interest in MSC fate specification because SNAI1 recruits histone demethylase KDM1A to the gene promoters resulting in a decrease in demethylated H3K4 levels to repress transcription. In addition, *SNAI1* is known to transcriptionally repress ectodermal genes within the mesoderm, formation and maintenance of embryonic mesoderm, and induction of the epithelial to mesenchymal transition[39].[40] Given the functional plasticity of miR-199a-5p in MSC terminal fate specification (Table 1), candidate gene evaluation for functionality should be supplemented with high throughput studies to perform an unbiased analysis of transcripts bound for silencing by miR-199a-5p in the RNA-induced silencing complex.

In addition to the miR-199 cluster (miR-199a-5p and miR-199a-3p), the precursor gene lncRNA *DNM3OS* also harbors the miR214 cluster (miR-214-5p and miR-214-3p). Since the miR-214 locus is 6 kb further downstream of the *MIR199A2* promoter, it remains to be determined whether its expression is regulated by the same proxy SNPs that contacts the *DNM3OS* and *MIR199A2* promoter; and whether modulating its activity during osteochondral fate specification of hMSC produces comparable results to that observed with miR-199a-5p. Nevertheless, a number of studies have indicated its role during chondrocyte differentiation[41][42],[43] and it is quite plausible that there is functional plasticity among the mature microRNAs originating from the *DNM3OS* and should be addressed for osteochondral fate specification of human progenitor cells in future studies. With regards to miR-199a-5p and miR-199a-3p, the contextual stability of mature microRNAs could be important in bone and cartilage homeostasis because existing literature supports negative regulation of chondrogenesis by miR-199a-3p in cellular models[11,15] and during ageing and osteoarthritis.[11,15] On the other hand, decreased miR-199a-5p expression was detected

Table 1. Experimentally validated miR-199a-5p and miR-199a-3p targets relevant for bone, cartilage and MSC.

S. No	Target	Cell/Tissue	miR-199a-5p or miR-199a-3p effect	Reference
miR-199a-5p				
1	IFIT2	Human stem cells from apical papilla (hSCAP)	miR-199a-5p transfected hSCAPs loaded onto beta-tricalcium phosphate scaffolds induced robust subcutaneous ectopic bone formation in vivo	44
2	TET2	Human bone marrow stromal cells	Over-expression of miR-199a-5p augmented ALP activity with enhanced calcification	45
3	HIFA; TWIST1	Wharton's jelly derived MSC	Chitosan nanoparticles/hsa miR-199a-5p agomir enhanced ectopic bone formation	46
4	IHH	Primary human chondrocytes	miR-199a-5p reduced chondrocyte hypertrophy and matrix degradation	12
5	MAPK4	Rat chondrocytes	miR-199a-5p inhibition increased proliferation and survival of chondrocytes	17
6	TGFBI	Human bone marrow stromal cells from aplastic anemia patients	PPAR-gamma regulated miR-199a-5p promoted BM-MSC adipogenesis	54
7	SHH	Chick embryo	miR-199 family upregulation resulted in smaller nasal pits and narrower face; miR-199 inhibition resulted in wider faces	55
8	MAFB	RAW 264.7 and macrophages	miR-199a-5p positively regulated RANKL-induced osteoclast differentiation	56
9	PIAS3, p27	Human osteosarcoma cells Saos-2 and MNNG/HOS	Inhibition of miR-199a-5p led to significant decrease in cell proliferation and tumor growth	57
10	VEGFA	Human osteosarcoma HOS cells	miR-199a-5p inhibited tumorigenesis and angiogenesis of HOS cells in vivo	58
miR-199a-3p				
1	KDM3A	Bone marrow stromal cells from OVX rats	miR-199a-3p increased in OVX rats to decrease osteogenesis	16
2	SMAD1	C3H10T1/2 cells	miR-199* inhibited early chondrogenesis by inhibiting Smad1/Smad4-mediated transactivation of target genes	15
3	DNMT3A	cartilage cells from knee osteoarthritis (KOA) rats	miR-199a-3p mimic decreased KOA chondrocyte apoptosis and promoted proliferation	59
4	RB1	Rheumatoid arthritis – fibroblast like synoviocytes (RA-FLS)	Ectopic miR-199a-3p expression significantly inhibited RA-FLS proliferation and induced apoptosis	60
5	IGF-1, mTOR	Osteocyte like MLO-Y4 cells	miR-199a-3p induced autophagy by modulating estrogen regulatory networks	61
6	KDM6A	Mouse bone marrow stromal cells (BM-MSC)	miR-199a-3p regulated adipogenesis by targeting KDM6A/WNT signaling	14
7	mTOR, MET, STAT3, MCL-1, BCL-X_L	Human osteosarcoma cell lines KHOS and U-2OS	miR-199a-3p expression reduced cell growth and migration	62
8	CD44	Human osteosarcoma cell lines KHOS and U-2OS	miR-199a-3p expression increased doxorubicin sensitivity; miR-199a-3p expression is significantly less in osteosarcoma compared to osteoblasts	63

in damaged articular cartilage tissues among osteoarthritis patients and intra-articular injection of synthetic miR-199a-5p agomir attenuated OA symptoms in rats including the alleviation of articular cartilage destruction, subchondral bone degradation, and synovial inflammation.[12] Three studies from human cell models, however, have shown increased osteoblast differentiation in miR-199a-5p over-expressing cells which could be attributed to different differentiation approach compared to this study.[44-46] Intriguingly, for TGF-β-responsive microRNAs such as miR-199a-5p, activated SMAD proteins are known to promote their post-transcriptional maturation through specific sequences (5'-CAGAC-3') within the pri-miRNA stem region that are on average 10 bp from the terminal loop. The presence of these SMAD binding sites, which are conserved both in human and mice miR-199a-5p, facilitates recruitment of Drosha and DGCR8 for their processing into mature forms.[47] Therefore, it would be interesting to evaluate in future studies how/whether mature miR-199a family expression changes with age and pathological conditions to implicate functional consequences in bone and cartilage.

The contextual upregulation and downregulation of *DNM3OS* and *MIR199A2* during chondrogenesis and osteoblastogenesis also warrants future investigations to understand the precise mechanism by which their putative promoters interact with the GWAS proxy SNPs. Both mouse and human studies have shown that the transcription factors TWIST1 and EGR1 regulate *DNM3OS* expression in a tissue- and development stage specific manner.[48] In umbilical cord derived human MSC, hypoxia induced *HIFA-TWIST1* pathways to upregulate miR-199a-5p at early stages of differentiation, while at late stages, miR-199a-5p enhanced osteogenesis maturation by inhibiting the *HIFA-TWIST* pathway.[46] Although, miR199a-5p expression closely

resembled the expression pattern of *DNM3OS* in our studies and that from Watanabe et al.,[9] the putative promoter for *MIR199A2* on chromosome 1 falls within a relatively CpG poor region that extends 81 bp–1349 bp upstream of the 5' end of the miRNA hairpin region.[49] Studies in several cell lines showed that this region is hypermethylated in cancer cells but hypomethylated in normal fibroblasts.[10] A study in murine cardiac myocytes showed that this promoter activity is further repressed by Stat3.[50] The post-transcriptional regulation of these microRNAs has been documented in liver injury and cardiac hypertrophy models where signals through β-adrengeric receptor favored their expression[51,52] but farnesoid X receptor activation[53] and AKT activation during hypoxia downregulated them.[52] Collectively, signals that modulate miR-199a-5p and miR-199a-3p expression appears to be tissue and context dependent. This can also be inferred from our data as a significant decrease in miR-199a-5p occurred after 24 h of BMP2 treatment during monolayer osteoblastogenesis (Figure 1C and D) and required 4 days to increase its expression during chondrogenesis (Figure 6B)—suggesting that the integration of BMP2 and TGF-β signals onto a secondary signal could be important for miR-199a-5p expression. This is further supported by our previous data where we have shown that the maximal SMAD1/5/9 phosphorylation is detected around 1–2 h post BMP-stimulation and corresponds with high levels of canonical BMP/SMAD target gene *ID1* expression at ~8 h that gradually returns to baseline over the next 3 days.[18] Furthermore, no SMAD binding sites are computationally predicted both within the proximal *DNM3OS* and *MIR199A2* promoter regions as well as the chromatin region harboring the four GWAS proxy variants. Therefore, understanding how/whether integration of BMP2 and TGF-β signals onto subsequent downstream pathways would provide mechanistic insight regarding both the regulation of *DNM3OS* and miR-199a-5p and the underlying molecular mechanism of terminal fate specification.

Dysregulation of terminal fate specification of MSC into chondrocytes or osteoblasts encompasses the basis of many musculoskeletal pathologies. Therefore, therapeutic interventions for musculoskeletal pathologies contextually require tools to program/reprogram progenitor cells into the desired terminal fate. miR-199a-5p is an attractive GWAS validated candidate gene for preclinical evaluation because of its ease to be contextually evaluated for various therapeutic approaches using cell programmable biomaterial scaffolds, direct gene delivery using nanoparticles, or in autologous cell-based therapies. miR-199a-5p mimic could be used to preserve cartilage turnover in joint diseases, while reducing its activity could be beneficial to address craniofacial skeletal defects where excessive cartilage formation is undesirable. In conclusion, our study sets a solid foundation for further characterization of this miRNA's role in BMD determination in vivo by defining its mechanistic role and to understand its genetic regulation through cis regulatory elements during cell fate specification.

Acknowledgments

Some of the materials employed in this work were provided by the Texas A&M Health Science Center College of Medicine Institute for Regenerative Medicine (IRM) at Scott & White through a grant from ORIP of the NIH, Grant # P40OD011050. We would like to dedicate this work to the founding director of the IRM at Texas A&M, Dr. Darwin Prockop (1929–2024), whose pioneering work in the field of progenitor cell and extracellular matrix biology has inspired many of our work. Cells used for chondrogenic pellet assays were obtained from Case Western University through a NIH/NIBIB funded P41: 1P41EB021911.

Author contributions

Gurcharan Kaur (Data curation, Formal analysis, Investigation), James A. Pippin (Data curation, Writing—original draft, Writing—review & editing), Solomon Chang (Data curation, Investigation), Justin Redmond (Data curation, Investigation), Alessandra Chesi (Data curation, Formal analysis, Investigation, Writing—original draft, Writing—review & editing), Andrew D. Wells (Data curation, Formal analysis, Project administration, Writing—original draft, Writing—review & editing), Tristan Maerz (Data curation, Formal analysis, Methodology, Supervision, Writing—original draft, Writing—review & editing), Struan F.A. Grant (Conceptualization, Formal analysis, Funding acquisition, Project administration, Supervision, Writing—original draft, Writing—review & editing), Rhima M. Coleman (Conceptualization, Formal analysis, Funding acquisition, Project administration, Resources, Supervision, Writing—original draft, Writing—review & editing), Kurt D. Hankenson (Conceptualization, Formal analysis, Funding acquisition, Methodology, Project administration, Resources, Supervision, Writing—original draft, Writing—review & editing), Yadav Wagley (Conceptualization, Data curation, Formal analysis, Investigation, Methodology, Supervision, Validation, Writing—original draft, Writing—review & editing).

Supplementary material

Supplementary material is available at *JBMR Plus* online.

Funding

This work was in part funded by the NIH Grant R01-AG072705-1. S.F.A.G is funded by the Daniel B. Burke Endowed Chair for Diabetes Research. K.D.H. is funded by the Henry Ruppenthal Family Endowed Professorship.

Conflicts of interest

None declared.

Data availability

All the data associated with this publication will be made available upon reasonable request.

References

1. Sozen T, Ozisik L, Basaran NC. An overview and management of osteoporosis. *Eur J Rheumatol*. 2017;4(1):46–56. https://doi.org/10.5152/eurjrheum.2016.048
2. Wright NC, Looker AC, Saag KG, et al. The recent prevalence of osteoporosis and low bone mass in the United States based on bone mineral density at the femoral neck or lumbar spine. *J Bone Miner Res*. 2014;29(11):2520–2526. https://doi.org/10.1002/jbmr.2269
3. Morris JA, Kemp JP, Youlten SE, et al. Author correction: an atlas of genetic influences on osteoporosis in humans and mice. *Nat Genet*. 2019;51(5):920. https://doi.org/10.1038/s41588-019-0415-x
4. Zhu X, Bai W, Zheng H. Twelve years of GWAS discoveries for osteoporosis and related traits: advances, challenges and applications. *Bone Res*. 2021;9(1):23. https://doi.org/10.1038/s41413-021-00143-3

5. Farber CR. Systems genetics: a novel approach to dissect the genetic basis of osteoporosis. *Curr Osteoporos Rep*. 2012;10(3):228–235. https://doi.org/10.1007/s11914-012-0112-5
6. Chesi A, Wagley Y, Johnson ME, et al. Genome-scale capture C promoter interactions implicate effector genes at GWAS loci for bone mineral density. *Nat Commun*. 2019;10(1):1260. https://doi.org/10.1038/s41467-019-09302-x
7. Pippin JA, Chesi A, Wagley Y, et al. CRISPR-Cas9-mediated genome editing confirms EPDR1 as an effector gene at the BMD GWAS-implicated 'STARD3NL' locus. *JBMR Plus*. 2021;5(9):e10531. https://doi.org/10.1002/jbm4.10531
8. Scott H, Howarth J, Lee YB, et al. MiR-3120 is a mirror microRNA that targets heat shock cognate protein 70 and auxilin messenger RNAs and regulates clathrin vesicle uncoating. *J Biol Chem*. 2012;287(18):14726–14733. https://doi.org/10.1074/jbc.M111.326041
9. Watanabe T, Sato T, Amano T, et al. Dnm3os, a non-coding RNA, is required for normal growth and skeletal development in mice. *Dev Dyn*. 2008;237(12):3738–3748. https://doi.org/10.1002/dvdy.21787
10. Wang Q, Ye B, Wang P, Yao F, Zhang C, Yu G. Overview of microRNA-199a regulation in cancer. *Cancer Manag Res*. 2019;Volume 11:10327–10335. https://doi.org/10.2147/CMAR.S231971
11. Ukai T, Sato M, Akutsu H, Umezawa A, Mochida J. MicroRNA-199a-3p, microRNA-193b, and microRNA-320c are correlated to aging and regulate human cartilage metabolism. *J Orthop Res*. 2012;30(12):1915–1922. https://doi.org/10.1002/jor.22157
12. Huang L, Jin M, Gu R, et al. miR-199a-5p reduces chondrocyte hypertrophy and attenuates osteoarthritis progression via the Indian hedgehog signal pathway. *J Clin Med*. 2023;12(4):1313. https://doi.org/10.3390/jcm12041313
13. Zhang Z, Kang Y, Zhang Z, et al. Expression of microRNAs during chondrogenesis of human adipose-derived stem cells. *Osteoarthr Cartil*. 2012;20(12):1638–1646. https://doi.org/10.1016/j.joca.2012.08.024
14. Shuai Y, Yang R, Mu R, Yu Y, Rong L, Jin L. MiR-199a-3p mediates the adipogenic differentiation of bone marrow-derived mesenchymal stem cells by regulating KDM6A/WNT signaling. *Life Sci*. 2019;220:84–91. https://doi.org/10.1016/j.lfs.2019.01.051
15. Lin EA, Kong L, Bai XH, Luan Y, Liu CJ. miR-199a, a bone morphogenic protein 2-responsive MicroRNA, regulates chondrogenesis via direct targeting to Smad1. *J Biol Chem*. 2009;284(17):11326–11335. https://doi.org/10.1074/jbc.M807709200
16. Wu JC, Sun J, Xu JC, Zhou ZY, Zhang YF. Down-regulated microRNA-199a-3p enhances osteogenic differentiation of bone marrow mesenchymal stem cells by targeting Kdm3a in ovariectomized rats. *Biochem J*. 2021;478(4):721–734. https://doi.org/10.1042/BCJ20200314
17. Lu H, Yang Y, Ou S, et al. The silencing of miR-199a-5p protects the articular cartilage through MAPK4 in osteoarthritis. *Ann Transl Med*. 2022;10(10):601. https://doi.org/10.21037/atm-22-2057
18. Wagley Y, Chesi A, Acevedo PK, et al. Canonical notch signaling is required for bone morphogenetic protein-mediated human osteoblast differentiation. *Stem Cells*. 2020;38(10):1332–1347. https://doi.org/10.1002/stem.3245
19. Wu B, Durisin EK, Decker JT, Ural EE, Shea LD, Coleman RM. Phosphate regulates chondrogenesis in a biphasic and maturation-dependent manner. *Differentiation*. 2017;95:54–62. https://doi.org/10.1016/j.diff.2017.04.002
20. Statello L, Guo CJ, Chen LL, Huarte M. Gene regulation by long non-coding RNAs and its biological functions. *Nat Rev Mol Cell Biol*. 2021;22(2):96–118. https://doi.org/10.1038/s41580-020-00315-9
21. Catalanotto C, Cogoni C, Zardo G. MicroRNA in control of gene expression: an overview of nuclear functions. *Int J Mol Sci*. 2016;17(10):1712. https://doi.org/10.3390/ijms17101712
22. Goldring MB. Human chondrocyte cultures as models of cartilage-specific gene regulation. *Methods Mol Med*. 2005;107:69–95.
23. Dishowitz MI, Zhu F, Sundararaghavan HG, Ifkovits JL, Burdick JA, Hankenson KD. Jagged1 immobilization to an osteoconductive polymer activates the notch signaling pathway and induces osteogenesis. *J Biomed Mater Res A*. 2014;102(5):1558–1567. https://doi.org/10.1002/jbm.a.34825
24. Zhu F, Sweetwyne MT, Hankenson KD. PKCdelta is required for Jagged-1 induction of human mesenchymal stem cell osteogenic differentiation. *Stem Cells*. 2013;31(6):1181–1192. https://doi.org/10.1002/stem.1353
25. Johnstone B, Hering TM, Caplan AI, Goldberg VM, Yoo JU. In vitro chondrogenesis of bone marrow-derived mesenchymal progenitor cells. *Exp Cell Res*. 1998;238(1):265–272. https://doi.org/10.1006/excr.1997.3858
26. Zou ML, Chen ZH, Teng YY, et al. The Smad dependent TGF-beta and BMP Signaling pathway in bone Remodeling and therapies. *Front Mol Biosci*. 2021;8:593310. https://doi.org/10.3389/fmolb.2021.593310
27. Kopf J, Petersen A, Duda GN, Knaus P. BMP2 and mechanical loading cooperatively regulate immediate early signalling events in the BMP pathway. *BMC Biol*. 2012;10(1):37. https://doi.org/10.1186/1741-7007-10-37
28. Galea GL, Zein MR, Allen S, Francis-West P. Making and shaping endochondral and intramembranous bones. *Dev Dyn*. 2021;250(3):414–449. https://doi.org/10.1002/dvdy.278
29. Sabik OL, Farber CR. Using GWAS to identify novel therapeutic targets for osteoporosis. *Transl Res*. 2017;181:15–26. https://doi.org/10.1016/j.trsl.2016.10.009
30. Cousminer DL, Wagley Y, Pippin JA, et al. Genome-wide association study implicates novel loci and reveals candidate effector genes for longitudinal pediatric bone accrual. *Genome Biol*. 2021;22(1):1. https://doi.org/10.1186/s13059-020-02207-9
31. Lefebvre V, Dvir-Ginzberg M. SOX9 and the many facets of its regulation in the chondrocyte lineage. *Connect Tissue Res*. 2017;58(1):2–14. https://doi.org/10.1080/03008207.2016.1183667
32. Au TYK, Yip RKH, Wynn SL, et al. Hypomorphic and dominant-negative impact of truncated SOX9 dysregulates hedgehog-Wnt signaling, causing campomelia. *Proc Natl Acad Sci USA*. 2023;120(1):e2208623119. https://doi.org/10.1073/pnas.2208623119
33. Zhao C, Jiang W, Zhou N, et al. Corrigendum to "Sox9 augments BMP2-induced chondrogenic differentiation by downregulating Smad7 in mesenchymal stem cells (MSCs)" [Genes & Diseases 4 (2017) 229-239]. *Genes Dis*. 2023;10(2):624–626. https://doi.org/10.1016/j.gendis.2023.02.003
34. Dash S, Trainor PA. The development, patterning and evolution of neural crest cell differentiation into cartilage and bone. *Bone*. 2020;137:115409. https://doi.org/10.1016/j.bone.2020.115409
35. Guasto A, Cormier-Daire V. Signaling pathways in bone development and their related skeletal dysplasia. *Int J Mol Sci*. 2021;22(9):4321. https://doi.org/10.3390/ijms22094321
36. Olivares-Navarrete R, Raz P, Zhao G, et al. Integrin alpha2beta1 plays a critical role in osteoblast response to micron-scale surface structure and surface energy of titanium substrates. *Proc Natl Acad Sci USA*. 2008;105(41):15767–15772. https://doi.org/10.1073/pnas.0805420105
37. Enomoto M, Leboy PS, Menko AS, Boettiger D. Beta 1 integrins mediate chondrocyte interaction with type I collagen, type II collagen, and fibronectin. *Exp Cell Res*. 1993;205(2):276–285. https://doi.org/10.1006/excr.1993.1087
38. Olivares-Navarrete R, Lee EM, Smith K, et al. Substrate stiffness controls osteoblastic and Chondrocytic differentiation of mesenchymal stem cells without exogenous stimuli. *PLoS One*. 2017;12(1):e0170312. https://doi.org/10.1371/journal.pone.0170312
39. Lin Y, Wu Y, Li J, et al. The SNAG domain of Snail1 functions as a molecular hook for recruiting lysine-specific demethylase 1.

EMBO J. 2010;29(11):1803–1816. https://doi.org/10.1038/emboj.2010.63
40. Lin T, Ponn A, Hu X, Law BK, Lu J. Requirement of the histone demethylase LSD1 in Snai1-mediated transcriptional repression during epithelial-mesenchymal transition. *Oncogene*. 2010;29(35):4896–4904. https://doi.org/10.1038/onc.2010.234
41. Roberto VP, Gavaia P, Nunes MJ, Rodrigues E, Cancela ML, Tiago DM. Evidences for a new role of miR-214 in Chondrogenesis. *Sci Rep*. 2018;8(1):3704. https://doi.org/10.1038/s41598-018-21735-w
42. Li QS, Meng FY, Zhao YH, Jin CL, Tian J, Yi XJ. Inhibition of microRNA-214-5p promotes cell survival and extracellular matrix formation by targeting collagen type IV alpha 1 in osteoblastic MC3T3-E1 cells. *Bone Joint Res*. 2017;6(8):464–471. https://doi.org/10.1302/2046-3758.68.BJR-2016-0208.R2
43. Cao Y, Tang S, Nie X, et al. Decreased miR-214-3p activates NF-kappaB pathway and aggravates osteoarthritis progression. *EBioMedicine*. 2021;65:103283. https://doi.org/10.1016/j.ebiom.2021.103283
44. Hu J, Huang X, Zheng L, et al. MiR-199a-5P promotes osteogenic differentiation of human stem cells from apical papilla via targeting IFIT2 in apical periodontitis. *Front Immunol*. 2023;14:1149339. https://doi.org/10.3389/fimmu.2023.1149339
45. Qi XB, Jia B, Wang W, et al. Role of miR-199a-5p in osteoblast differentiation by targeting TET2. *Gene*. 2020;726:144193. https://doi.org/10.1016/j.gene.2019.144193
46. Chen X, Gu S, Chen BF, et al. Nanoparticle delivery of stable miR-199a-5p agomir improves the osteogenesis of human mesenchymal stem cells via the HIF1a pathway. *Biomaterials*. 2015;53:239–250. https://doi.org/10.1016/j.biomaterials.2015.02.071
47. Davis BN, Hilyard AC, Nguyen PH, Lagna G, Hata A. Smad proteins bind a conserved RNA sequence to promote microRNA maturation by Drosha. *Mol Cell*. 2010;39(3):373–384. https://doi.org/10.1016/j.molcel.2010.07.011
48. Lee YB, Bantounas I, Lee DY, Phylactou L, Caldwell MA, Uney JB. Twist-1 regulates the miR-199a/214 cluster during development. *Nucleic Acids Res*. 2009;37(1):123–128. https://doi.org/10.1093/nar/gkn920
49. Fujita S, Iba H. Putative promoter regions of miRNA genes involved in evolutionarily conserved regulatory systems among vertebrates. *Bioinformatics*. 2008;24(3):303–308. https://doi.org/10.1093/bioinformatics/btm589
50. Haghikia A, Missol-Kolka E, Tsikas D, et al. Signal transducer and activator of transcription 3-mediated regulation of miR-199a-5p links cardiomyocyte and endothelial cell function in the heart: a key role for ubiquitin-conjugating enzymes. *Eur Heart J*. 2011;32(10):1287–1297. https://doi.org/10.1093/eurheartj/ehq369
51. Park KM, Teoh JP, Wang Y, et al. Carvedilol-responsive microRNAs, miR-199a-3p and -214 protect cardiomyocytes from simulated ischemia-reperfusion injury. *Am J Physiol Heart Circ Physiol*. 2016;311(2):H371–H383. https://doi.org/10.1152/ajpheart.00807.2015
52. Rane S, He M, Sayed D, Yan L, Vatner D, Abdellatif M. An antagonism between the AKT and beta-adrenergic signaling pathways mediated through their reciprocal effects on miR-199a-5p. *Cell Signal*. 2010;22(7):1054–1062. https://doi.org/10.1016/j.cellsig.2010.02.008
53. Balasubramaniyan N, Devereaux MW, Orlicky DJ, Sokol RJ, Suchy FJ. miR-199a-5p inhibits the expression of ABCB11 in obstructive cholestasis. *J Biol Chem*. 2021;297(6):101400. https://doi.org/10.1016/j.jbc.2021.101400
54. Zhang X, Liu L, Dou C, et al. PPAR gamma-regulated MicroRNA 199a-5p underlies bone marrow adiposity in aplastic Anemia. *Mol Ther Nucleic Acids*. 2019;17:678–687. https://doi.org/10.1016/j.omtn.2019.07.005
55. Richbourg HA, Hu DP, Xu Y, Barczak AJ, Marcucio RS. miR-199 family contributes to regulation of sonic hedgehog expression during craniofacial development. *Dev Dyn*. 2020;249(9):1062–1076. https://doi.org/10.1002/dvdy.191
56. Guo K, Zhang D, Wu H, Zhu Q, Yang C, Zhu J. MiRNA-199a-5p positively regulated RANKL-induced osteoclast differentiation by target Mafb protein. *J Cell Biochem*. 2019;120(5):7024–7031. https://doi.org/10.1002/jcb.27968
57. Wang C, Ba X, Guo Y, et al. MicroRNA-199a-5p promotes tumour growth by dual-targeting PIAS3 and p27 in human osteosarcoma. *Sci Rep*. 2017;7(1):41456. https://doi.org/10.1038/srep41456
58. Zhang L, Cao H, Gu G, et al. Exosomal MiR-199a-5p inhibits tumorigenesis and angiogenesis by targeting VEGFA in osteosarcoma. *Front Oncol*. 2022;12:884559. https://doi.org/10.3389/fonc.2022.884559
59. Gu W, Shi Z, Song G, Zhang H. MicroRNA-199-3p up-regulation enhances chondrocyte proliferation and inhibits apoptosis in knee osteoarthritis via DNMT3A repression. *Inflamm Res*. 2021;70(2):171–182. https://doi.org/10.1007/s00011-020-01430-1
60. Wangyang Y, Yi L, Wang T, et al. MiR-199a-3p inhibits proliferation and induces apoptosis in rheumatoid arthritis fibroblast-like synoviocytes via suppressing retinoblastoma 1. *Biosci Rep*. 2018;38(6):BSR20180982. https://doi.org/10.1042/BSR20180982
61. Fu J, Hao L, Tian Y, Liu Y, Gu Y, Wu J. miR-199a-3p is involved in estrogen-mediated autophagy through the IGF-1/mTOR pathway in osteocyte-like MLO-Y4 cells. *J Cell Physiol*. 2018;233(3):2292–2303. https://doi.org/10.1002/jcp.26101
62. Duan Z, Choy E, Harmon D, et al. MicroRNA-199a-3p is downregulated in human osteosarcoma and regulates cell proliferation and migration. *Mol Cancer Ther*. 2011;10(8):1337–1345. https://doi.org/10.1158/1535-7163.MCT-11-0096
63. Gao Y, Feng Y, Shen JK, et al. CD44 is a direct target of miR-199a-3p and contributes to aggressive progression in osteosarcoma. *Sci Rep*. 2015;5(1):11365. https://doi.org/10.1038/srep11365